# MODELING OF SMF TSUNAMI GENERATION AND REGIONAL IMPACT ALONG THE UPPER U.S. EAST COAST

BY

STEPHAN T. GRILLI, CHRISTOPHER O'REILLY

AND TAYEBEH TAJALLI BAKHSH

DEPT. OF OCEAN ENGINEERING, UNIVERSITY OF RHODE ISLAND

RESEARCH REPORT NO. CACR-13-05

NTHMP AWARD #NA10NWS4670010
NATIONAL WEATHER SERVICE PROGRAM OFFICE

CENTER FOR APPLIED COASTAL RESEARCH
Ocean Engineering Laboratory
University of Delaware
Newark, Delaware 19716

# Table of contents

# Table of Figures

# Introduction

The University of Delaware and the University of Rhode Island (URI) have been funded since 2010 by NOAA's NTHMP program to perform model simulations of tsunami generation, propagation and impact on the U.S. East Coast, in order to establish tsunami inundation maps of the region. Such studies first require the identification, selection, and parameterization of tsunami sources within the Atlantic Ocean Basin, an area that governs the east coast tsunami hazard (ten Brink et al., 2007, 2008; Grilli et al. 2011). Potential extreme far-field co-seismic sources are found in the Azores-Gibraltar convergence zone and the Hispanola-Puerto Rico-Lesser Antilles subduction zone areas (Grilli et al., 2010b, 2011). These would have the potential for creating up to M9 earthquakes that would trigger large transoceanic tsunamis. Furthermore, a large transoceanic tsunami could be triggered by the massive flank collapse (i.e., subaerial mass failure) of the Cumbre Vieja Volcano, in the Canary Islands (Abadie et al., 2010, 2012; Harris et al., 2012). These sources constitute the far- field tsunami risk for the U.S. east coast. They have been considered within the NTHMP project and have been discussed in other reports (Grilli and Grilli, 2013a,b,c).

A near-field tsunami threat is posed by tsunamigenic Submarine Mass Failures (SMF) that could be triggered by moderate seismic activity along the lower continental slope and upper rise of the western Atlantic Ocean. Earlier work (ten Brink et al., 2007, 2008, 2009a,b; Grilli et al., 2009) indicates that such sources may pose a significant tsunami hazard for the U.S. East Coast, albeit for more localized area for each SMF source than for co-seismic tsunamis (e.g., Watts et al., 2003; Grilli and Watts, 2005; Watts et al., 2005; Tappin et al., 2008; Grilli et al., 2009).

Although SMF triggered tsunamis are less energetic than large co-seismic tsunamis, they may occur in fairly shallow water, at a short distance from shore, which may cause significant runup along a localized section of the coast while offering little warning time. Although only a few historical landslide tsunamis have been clearly identified in the region, ten Brink et al. (2007) and Twichell et al. (2009) report that landslide scars cover a significant portion of the continental slope and rise along the U.S. East Coast and that many of these landslides are large in volume (above 100 $km^3$). A large SMF could generate runups of more than five meters on nearby coasts (Grilli et al., 2009), a hazard potentially surpassing the runup generated by a typical 100 year hurricane storm surge in the region.

While there is clear evidence of past large scale SMFs within our area of interest, the magnitude, location, volume and mode of rupture of those observed landslide scars is poorly known. As a result of this lack of data and uncertainties in identifying potential SMF source locations and their parameters, a Monte Carlo analysis was developed and applied by Grilli et al. (2009), in which distributions of relevant parameters (seismicity, sediment properties, and SMF type, location, geometry, etc.) were used to perform a large number of stochastic stability analyses of actual slope transects within the study area. This allowed computing statistical distributions of potential tsunamigenic SMFs and their expected 100 and 500 year runups, within an area initially spanning from New Jersey to Cape Cod. This analysis was later extended all the way south to Florida, and further

North to Maine (Krauss, 2011), identifying potential tsunamigenic sources within the entire NTHMP study area.

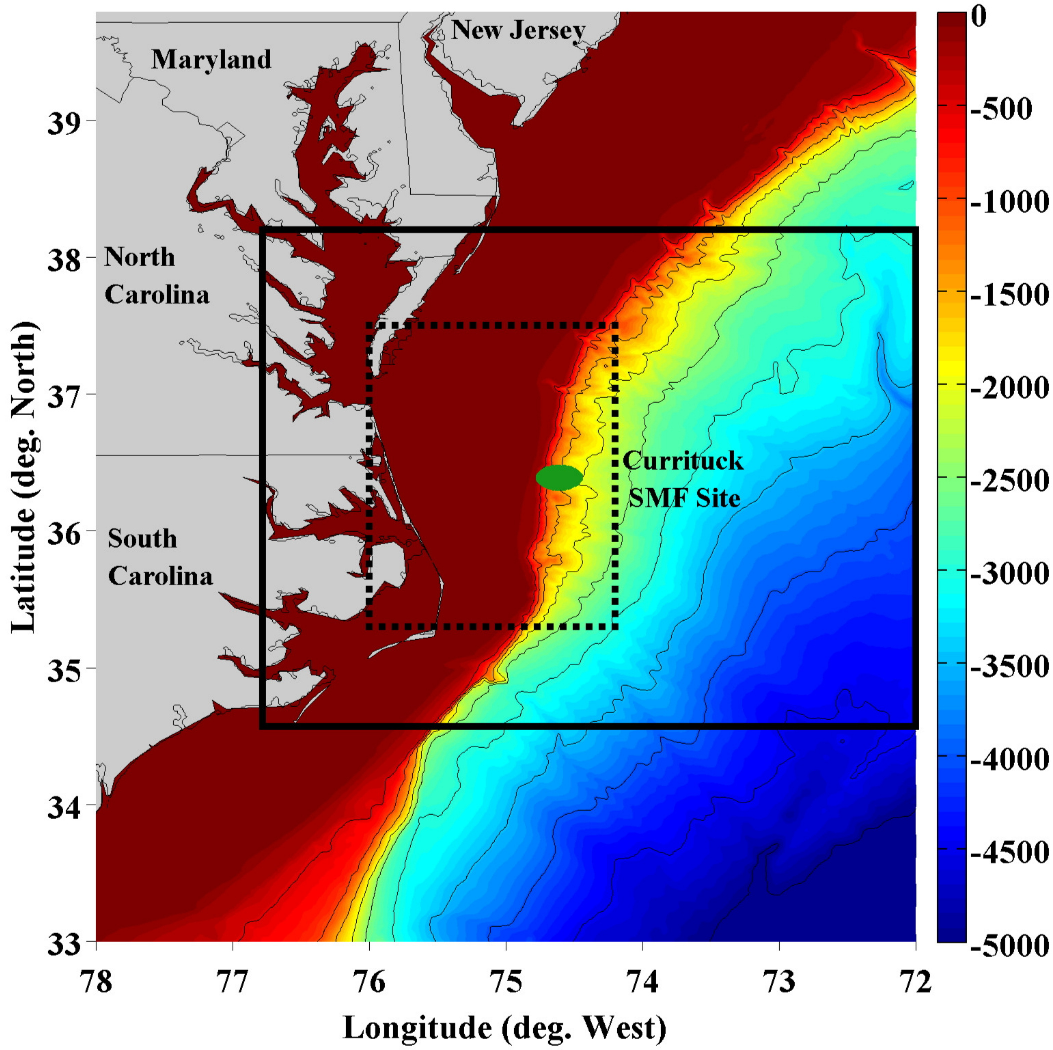


**Figure 1: Location Map of Currituck slide. Depth indicated in meters, in the color scale. The center of the Currituck SMF is at 74.61W and 36.39N (where 1 deg. in longitude is 89 km). The solid black box marks the boundary of the 500 m resolution grid (800 x 900 cells; lower left corner coordinates are: 76.8W and 34.6N) used in NHWAVE and FUNWAVE simulations and the dashed block box is a smaller zoomed in domain used later to visualize simulation results (lower left corner coordinates are: 76.0W and 35.3N).**

While this work provided potential SMF sites and estimates of SMF tsunami coastal impact, determining individual landslide characteristics at each site in order to perform more detailed tsunami generation and propagation simulations is difficult, because of the lack of available field data. As a result, it was decided in this project, and endorsed by the NTHMP Mapping and Modeling Subcommittee (MMS), to use a SMF similar to the historical Currituck slide (Figure 1) as a proxy to represent the potential worst case SMF scenario in the region. Grilli et al. (2009) showed that the highest-risk tsunami areas identified from New Jersey to Massachusetts show a reasonable potential for the occurrence of a Currituck type SMF and the most likely parameters of this SMF have been estimated in past work (Bunn and McGregor, 1980; Prior et al., 1986; and Locat et al., 2009).

Numerical modeling of tsunami generation and propagation associated with the Currituck SMF event was performed by several authors, including Geist et al. (2009), who used the dispersive weakly nonlinear Boussinesq model COULWAVE. They modeled the 2D (horizontal) Currituck tsunami wave field using a range of potential SMF movements, bounded by the mobility analysis of Locat et al. (2009), specified as a simplified free surface initial condition in the model. Additionally, a high resolution (5 m grid) and fully nonlinear 1D simulation of the Currituck tsunami was performed, highlighting the importance of wave breaking, dispersion, and nonlinearity in near shore propagation. Their results showed that nearshore runup is primarily affected by SMF volume, and then by failure duration. Grilli et al. (2013) performed similar 2D and 1D simulations using the Boussinesq model FUNWAVE-TVD (Shi et al., 2012). To simulate the SMF tsunami source generation, however, they used the fully three-dimensional (3D) non-hydrostatic sigma-layer model NHWAVE (Ma et al., 2012), in which the SMF motion was specified as a bottom boundary condition.

In the following, we first detail the parameterization and modeling of the historical Currituck event. This will include a new reconstruction of the geometry and kinematics of the slide and simulation of the resulting tsunami generation using NHWAVE, and propagation over the shelf to the coastline using FUNWAVE. Many sensitivities analyses to model and grid parameters are presented to ensure proper convergence and accuracy of SMF tsunami results. Present results are also discussed and compared to earlier published work. Finally, in preparation for FY13 work, we briefly model and discuss the impact of the Currituck event on the area of Virginia Beach and Norfolk, as well as the mouth of the Chesapeake Bay.

Next we parameterize and model tsunami generation, based on the same methodology (i.e., NHWAVE-FUNWAVE coupling) for four Currituck-like SMF sources in the high-risk SMF area identified by Grilli et al. (2009) from the Carolinas to Cape Cod. This area of the shelf and shelf break was studied in more detail from a geological and geotechnical point of view by Krause (2011) and Eggelling (2012) (e.g., from the point of view of sediment availability and stability). Based on these studies, 4 SMF locations were selected for further modeling, from Virginia to Eastern Long Island. Finally, the Cape Fear historical slide is modeled to provide the worst case SMF tsunami to impact the Myrtle Beach, SC area.

## Simulations of the Currituck SMF Tsunami

### Overall slide geometry and motion

The Currituck event consisted of a major submarine landslide, that occurred off of the coast of what is now North Carolina and Virginia, between 24 and 50 ka ago (Locat et al, 2009). It is the most prominent large scale SMF found along the western Atlantic Ocean continental slope and rise. Detailed descriptions of the stratigraphy and morphology of the Currituck submarine mass failure (SMF) have been reported on the basis of seismic surveys, by Bunn and McGregor (1980), Prior et al. (1986) and Locat et al. (2009). The latter work in particular presents a morpho-stratigraphic model of the failed mass and a depositional model of the run-out zone. Based on these works, the important tsunamigenic characteristics of the Currituck SMF may be inferred (Figure 2 and Figure 3).

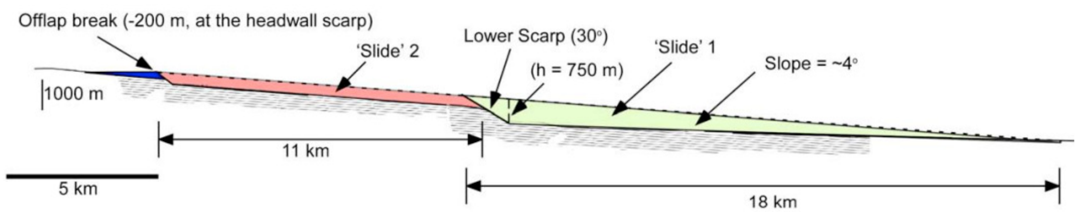


**Figure 2: Estimated transect of the pre-failed Currituck and the two sections of the landslide, Slide 1 (green) and Slide 2 (red) (Locat et al., 2009).**

Thus, it is found that the Currituck event consisted of two separate failed masses: Slide 1, which has an approximate 100 $km^3$ volume of sediment and Slide 2 which has a 60 $km^3$ volume. Locat et al. (2009) showed, based on its morphology and geometry, that the failure occurred rapidly, justifying that the Currituck SMF be modeled as a single failed mass for the purpose of tsunami generation. Here, it is assumed that the Currituck SMF had a maximum thickness of roughly $T$ = 750 m close to the center of the failed area (at $x_0$ = 74.7W and $y_0$ = 36.5N), a maximum down-slope length of $b$ = 30 km, and a maximum width of $w$ = 20 km (Figure 2 and Figure 3). At the Currituck site the headwall of Slide 2 begins at approximately a 500 m depth and is approximately 200 meters thick, roughly indicating the start of the landslide. Although parts of the SMF traveled for very large distances on the seafloor, to establish the SMF kinematics relevant to tsunami generation, we only consider the parameterization of the runout distance (and related time of motion) corresponding to the so-called tsunamigenic part of SMF motion; this is detailed later in this report. Finally, the SMF is assumed to have traveled due East or in azimuth $\theta$ = 90 deg.

Boundary conditions necessary to specify the SMF geometry and kinematics within NHWAVE were implemented following the modeling work of Grilli et al. (2002), Grilli and Watts (1999, 2005), Watts et al (2005), Enet et al. (2003), and Enet and Grilli

(2005, 2007). These served as the basis for defining the Currituck SMF geometry and motion in the present simulations.

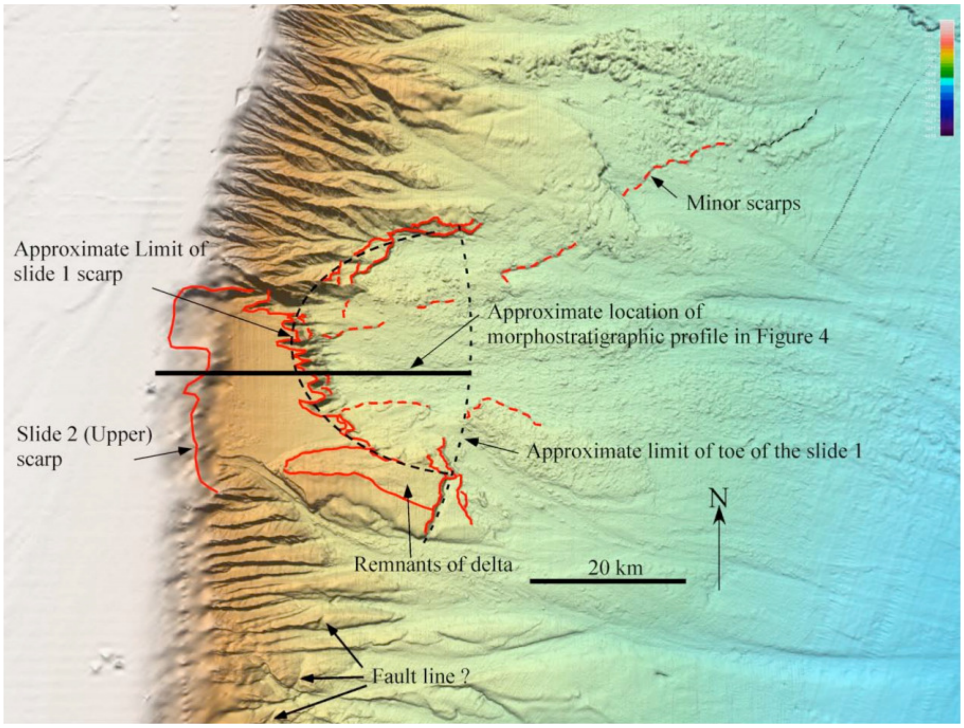


**Figure 3: Main morphological components of the Currituck SMF (Locat et al., 2009).**

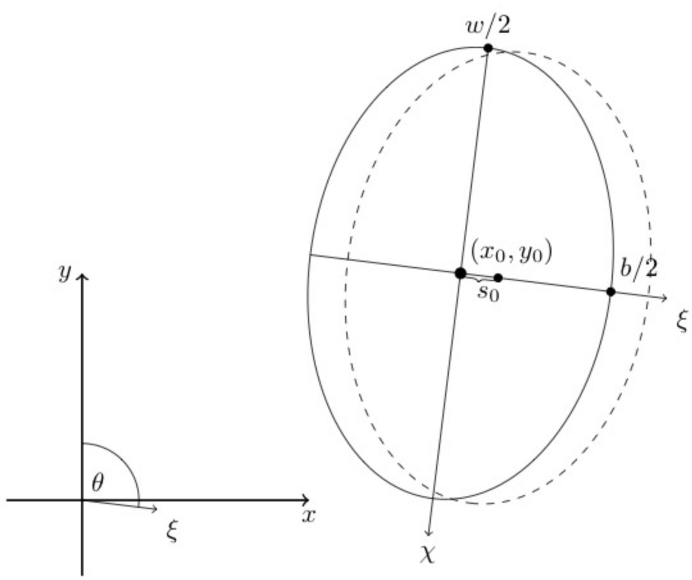


**Figure 4: Geometric parameterization of a SMF initially centered at *$(x_0, y_0)$* moving in direction $\xi$, with an azimuth angle $\theta$ from North and center of mass motion *$s(t)$; $(x,y)$* denote the latitudinal and longitudinal directions, respectively.**

More specifically, tsunami generation within NHWAVE considers a rigid SMF with a shape idealized as a "Gaussian" mound of elevation $\zeta$ and elliptical footprint (whose steepness is controlled by a shape parameter $\varepsilon$□, with an elliptical footprint, of length $b$, width $w$, and maximum thickness $T$ defined as (Figure 4),

$$\zeta(\xi,\chi)=\frac{T}{1-\varepsilon}\max\left[0,\ \operatorname{sech}(k_b\xi)\operatorname{sech}(k_w\chi)-\varepsilon\right]$$
$$k_b=\frac{2}{b}\operatorname{acosh}\frac{1}{\varepsilon}$$
$$k_w=\frac{2}{w}\operatorname{acosh}\frac{1}{\varepsilon}$$

(1)

where ($\xi,\chi$) are the local down-slope and span-wise coordinates, rotated to the direction of SMF motion $\theta$, and here $\varepsilon$ = 0.717 (Enet and Grilli, 2007). With this geometry and parameters, the SMF volume is found as,

$$V_b=bwT\left(\frac{f^2-\varepsilon}{1-\varepsilon}\right)\qquad \text{with}\qquad f=\frac{2}{C}\operatorname{atan}\sqrt{\frac{1-\varepsilon}{1+\varepsilon}}\quad \text{and}\quad C=\operatorname{acosh}\left(\frac{1}{\varepsilon}\right) \tag{2}$$

Using the slide dimensions given above, Eq. (2) yields the SMF simulated volume $V_b$ = 134 km$^3$ of sediment, which is in reasonable agreement with past geological work.

During its tsunamigenic period of motion, the modeled Currituck SMF is assumed to have a small maximum displacement (runout) $s_f$ in its direction of motion down the slope, over a time of motion $t_f$. The combination of rigid block SMF and small displacement parallel to the slope is similar to the kinematics of rigid rotational SMFs with constant basal friction (and negligible hydrodynamic drag) analyzed in previous work (see above-listed references), leading to a pendulum-like center of mass motion. In the absence of SMF observations, for the tsunami generation modeling, we elected to use this simple law of motion parameterized for an initial (triggering) time $t_i$ = 0, a characteristic period of motion $t_0$ (with $t_f = \pi t_0$), and a characteristic distance of motion $s_0$ (with $s_f = 2s_0$) as,

$$s(t)=\begin{cases} 0 & t<t_i \\ s_0\left(1-\cos\left\{\dfrac{t-t_i}{t_0}\right\}\right) & t_i\le t<t_i+\pi t_0 \\ 2s_0 & t_i+\pi t_0\le t \end{cases} \tag{3}$$

Unlike the simple planar slopes used in earlier numerical work and in laboratory experiments (Enet and Grilli, 2007), the bathymetry available here to locate the initial position of the SMF center of mass ($x_0$, $y_0$) and azimuth angle of motion $\theta$ (clockwise from north), leads us first to use the coordinate transformation (Figure 4),

$$\xi=(x-x_0)\cos\theta-(y-y_0)\sin\theta-s(t)$$
$$\chi=(x-x_0)\sin\theta+(y-y_0)\cos\theta$$

(4)

with $s(t)$ given by Eq. (3). Then, the instantaneous seafloor depth above the SMF is given by (with $\Delta h = h - h_0$),

$$h(x,y,t) = h_0(x,y) + \zeta\{\xi(x,y), \chi(x,y), t\} - \zeta\{\xi(x,y), \chi(x,y), t_i\} \tag{5}$$

where $h_0(x,y)$ is the existing local bathymetry (Figure 5), which for Currituck requires a reconstruction of the pre-event (pre-failed) conditions; this is detailed in the next section. This results in a motion that is equivalent to a horizontal translation of part of the seabed. The vertical seafloor velocity (used in NHWAVE as boundary condition) is then simply computed as,

$$\frac{dh}{dt}(x,y,t) = \frac{d}{dt}\{\zeta\{\xi(x,y,s(t)), \chi(x,y)\}\} \tag{6}$$

which can be easily derived from Eqs. (1-5).

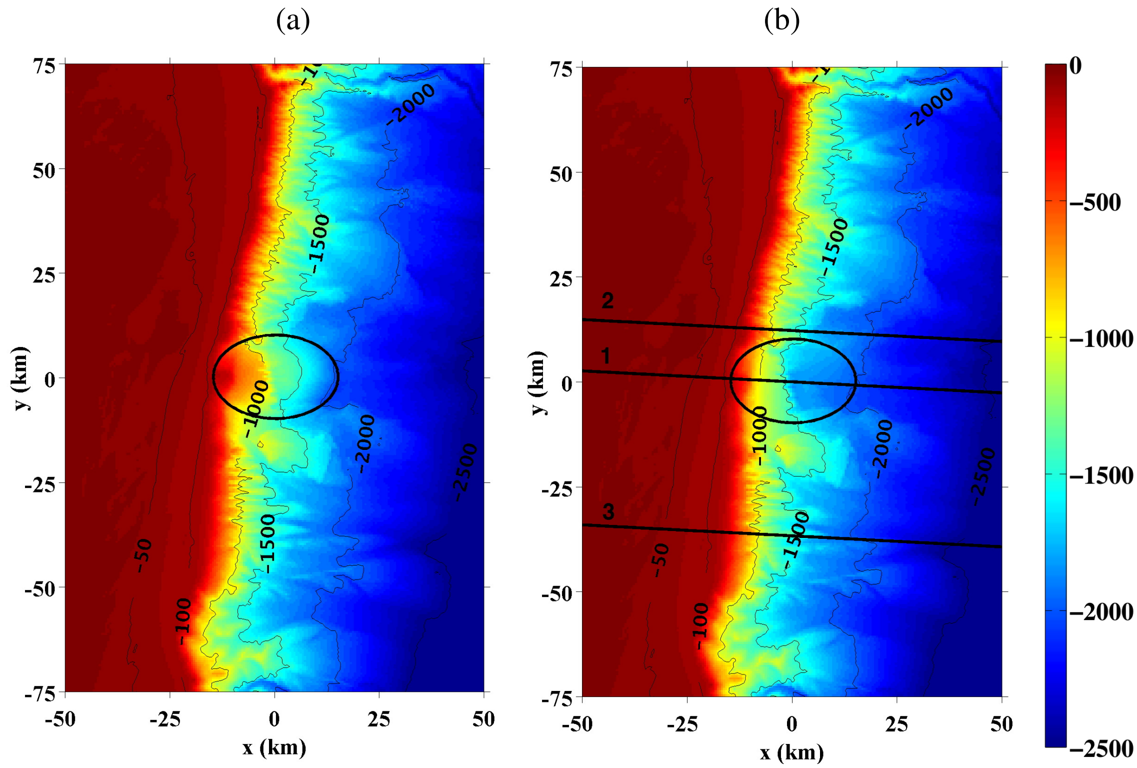


**Figure 5: Bathymetry at the Currituck site and surrounding area (color scale indicates depth in meters, ellipse is the SMF footprint, similar to Figure 1, and axes are distance measured from the SMF center at 74.61W and 36.39N): (a) reconstructed bathymetry; (b) current (post-failed) bathymetry with black lines marking bathymetric transects shown in Figure 6 (Currituck SMF central axis corresponds to transect 1).**

## Detailed Currituck slide geometry/bathymetry reconstruction

The simulation of the Currituck event requires reconstructing the pre-event (pre-failed) bathymetry, to be used in tsunami generation modeling, and hence to add the volume of sediment $V_b$ to the current post-failed area. However, a direct addition of a SMF described by Eq. (1) to the current bathymetry did not accurately reconstruct the failed slope as it was determined that during its motion the failed sediment from Slide 2 moved (flowed) into and partially filled the back of the cavity left by the slide (Prior et al., 1986).

Therefore part of the sediment within the reconstructed Currituck SMF consists of sediment currently at the site (i.e., sediment having flowed from Slide 2 into the back of Slide 1 beyond the tsunamigenic period). Specifically, here, reconstruction is done by first removing a 250 m thick SMF from the site, also described by Eq. (1) and with the same parameters as the full SMF (Figure 6 transect in dashed red). Then, before running simulations, NHWAVE adds the specified SMF shape with maximum thickness 750 m to the existing bathymetry (which brings the dashed red transect to the solid black transect in Figure 6).

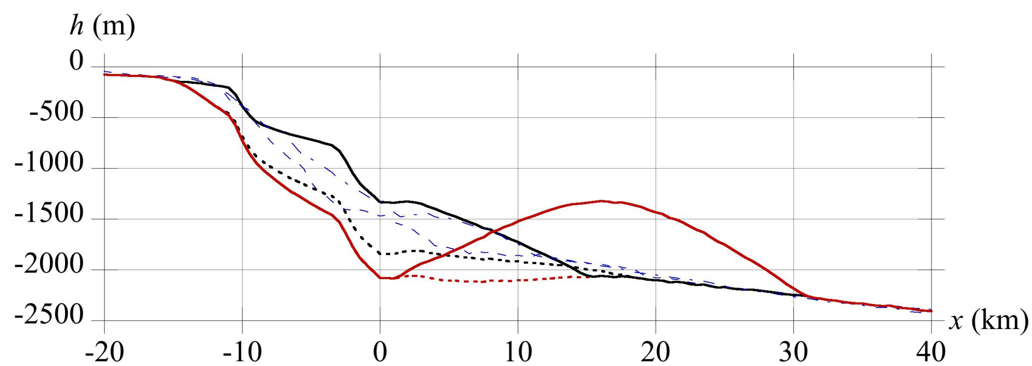


**Figure 6: Bathymetric transects through and adjacent to the center of the Currituck slide, marked in Figure 5: (- - -) existing post-failed bathymetry along the SMF direction of motion (transect 1); (-- --) existing post-failed bathymetry along transect 2; (-- - --) existing post-failed bathymetry along transect 3; (----) reconstructed pre-failed transect 1; (- - -) transect 1 with a Currituck SMF of 250 m max. thickness removed; and (----) transect 1 at the end of the SMF tsunamigenic motion duration, computed with Eqs. (3-5).**

As indicated, Figure 5 and Figure 6 illustrate the slope reconstruction of the Currituck SMF, relative to the surrounding area. Although the actual geometry of the Currituck SMF site is unknown (assumed of Gaussian shape here), the surrounding pre-failed geometry of the continental slope is. Figure 6 thus shows bathymetric transects 2 and 3 marked in Figure 5, which pass through areas north and south of the failure site; after reconstruction, we see that these two pre-failed profiles are consistent with each other. As discussed before, Figure 6 compares various transects through the center of the reconstructed Currituck site bathymetry to the neighboring transects 2 and 3. We see that the reconstructed Currituck transects has a bathymetry similar to its surrounding area, which should be expected (Locat et al., 2009). This could be further improved by the addition of small canyons, which however, would be inconsequential to tsunami generation.

Finally, Figure 6 shows transect 1 at the end of tsunamigenic part of SMF motion, which will be estimated below to be about 12 minutes. Beyond this time, while there will only be minor wave generation. Based on earlier work (Locat et al., 2009), it is assumed that the mound of sediment will keep spreading in all directions, mostly down the slope but also in the back of the SMF to fill part of the initial small cavity that was removed, prior to adding the SMF.

## Detailed Curritutck Slide Kinematics

As indicated before, the Currtiuck SMF is modeled as a rigid rotational failure, or slump, parameterized within NHWAVE using the equations of motion (3) derived by Grilli and Watts (2005), with the geometric parameterization (Eqs. (1-2)) of Enet and Grilli (2007). The SMF failure is represented by a rigid mass translating over an inclined plane, with center of mass motion *s(t)* (Figure 4) derived by balancing inertia, gravity, buoyancy, Coulomb friction, and hydrodynamic drag forces.

For slumps, the latter is neglected versus basal Coulomb friction (Grilli and Watts, 2005; Watts et al., 2005). Inertia includes both slide mass $M_b = \rho_b V_b$, with $\rho_b$ denoting slide bulk density and the specific density being defined as $\gamma = \rho_b/\rho_w$, with $\rho_w$ the water density, and an added mass $\Delta M_b = C_m \rho_w V_b$, defined by way of an added mass coefficient $C_m$.

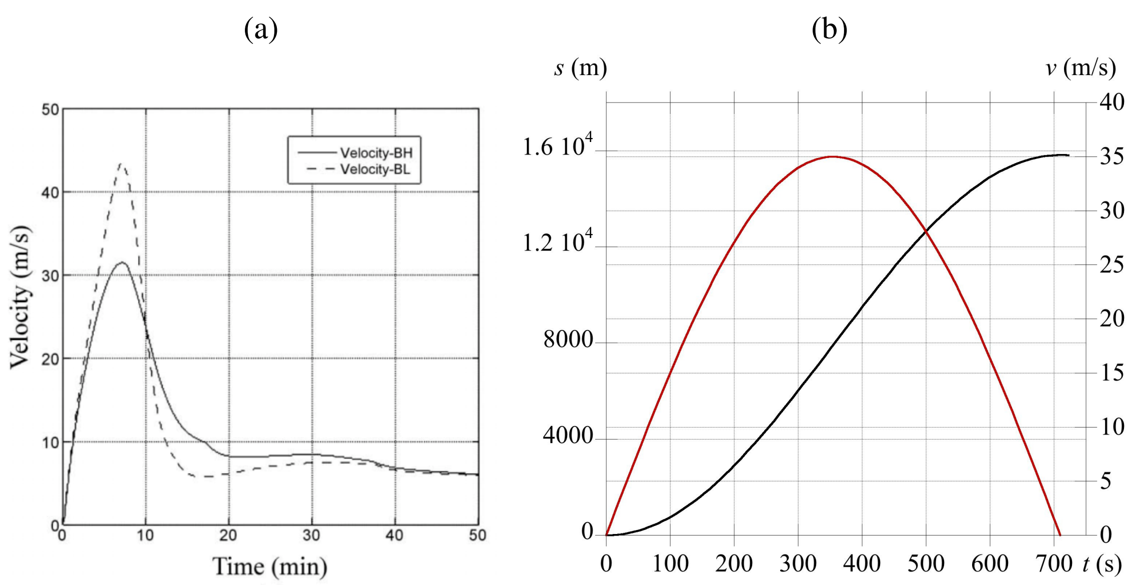


**Figure 7: (a) simulation of the Currituck slide frontal element velocity using two different deforming slide models (Locat et al., 2009); (b) proposed Currituck SMF (slump) motion *s* (----) and velocity *v* (----), for NTHMP simulations.**

Assuming a nearly circular rupture surface of radius $R$ and a small angular displacement $\Delta\phi$, we find for the characteristic distance and time of motion,

$$s_0 = \frac{R\Delta\phi}{2} \qquad \text{and} \quad t_0 = \sqrt{\frac{R}{g}\frac{\gamma + C_m}{\gamma - 1}} \tag{7}$$

with $g$ denoting the gravitational acceleration. Watts et al. (2005) proposed a semi-empirical relationship to obtain the radius of slump motion as a function of slump downslope length and maximum thickness as,

$$R \simeq \frac{b^2}{8T} \tag{8}$$

Assuming $\gamma = 1.85$ and $C_m = 1$, as in Grilli and Watts (2005), Eqs. (7) and (8) yield $R$ = 150 km and a characteristic time of motion $t_0$ = 226 s, resulting in an overall failure duration of $t_f$ = 11.9 minutes.

This time is consistent with the duration of the tsunamigenic slide motion inferred from the slide velocity profiles calculated by Locat et al (2009) and shown in Figure 7a. These authors used two types of deforming slide models to calculate the velocity of the Currituck slide frontal element. On this basis, they concluded that the peak slide velocity during the event was likely between 30 and 40 m/s. In the present simulations, since the distance traveled by the Currituck slide during the tsunamigenic part of its motion is unknown, we selected the slide runout $s_f$ and characteristic distance traveled $s_0$ such that, with $t_0$ = 226 s, the maximum slump velocity predicted by Eq. (3) match that of Locat et al. (2009), i.e., $v_{\max} = s_0/t_0 \approx 35$ m/s. This yields $s_0$ = 7910 m, or $s_f$ = 15.8 km, based on the law of motion in Eq. (3) (Figure 7b). This value yields $\Delta\phi =$ □□□□□□□□□□□□□□□□□□□□□, which is consistent with the assumed small angular displacement of a slump in the theory of Grilli and Watts (2005).

As indicated before, the final bathymetry computed using Eqs. (3-5) after tsunami generation is shown in Figure 6 (solid red transect). Beyond this point the SMF would have reached the lower velocity and acceleration region described by Locat et al. (2009), and disperse over the seafloor.

## Currituck SMF tsunami source generation and early propagation simulation

### SMF tsunami source generation with NHWAVE

The Currituck SMF tsunami source generation is simulated with NHWAVE, based on the geometry, bathymetry, and slump-like kinematics discussed in the previous sections (Figure 7b) over time $t_f$ = 710 s (11.9 min.). A 3D grid made of 3 sigma-layers and with a horizontal mesh having a 500 m resolution (or about 16 arc-second) is first used. The horizontal footprint of the computational domain, 400 by 450 km (with 800 x 900 cells), is marked in Figure 1, as well as a smaller area of 165.5 by 244 km over which we zoomed in to present results in some of the following figures.

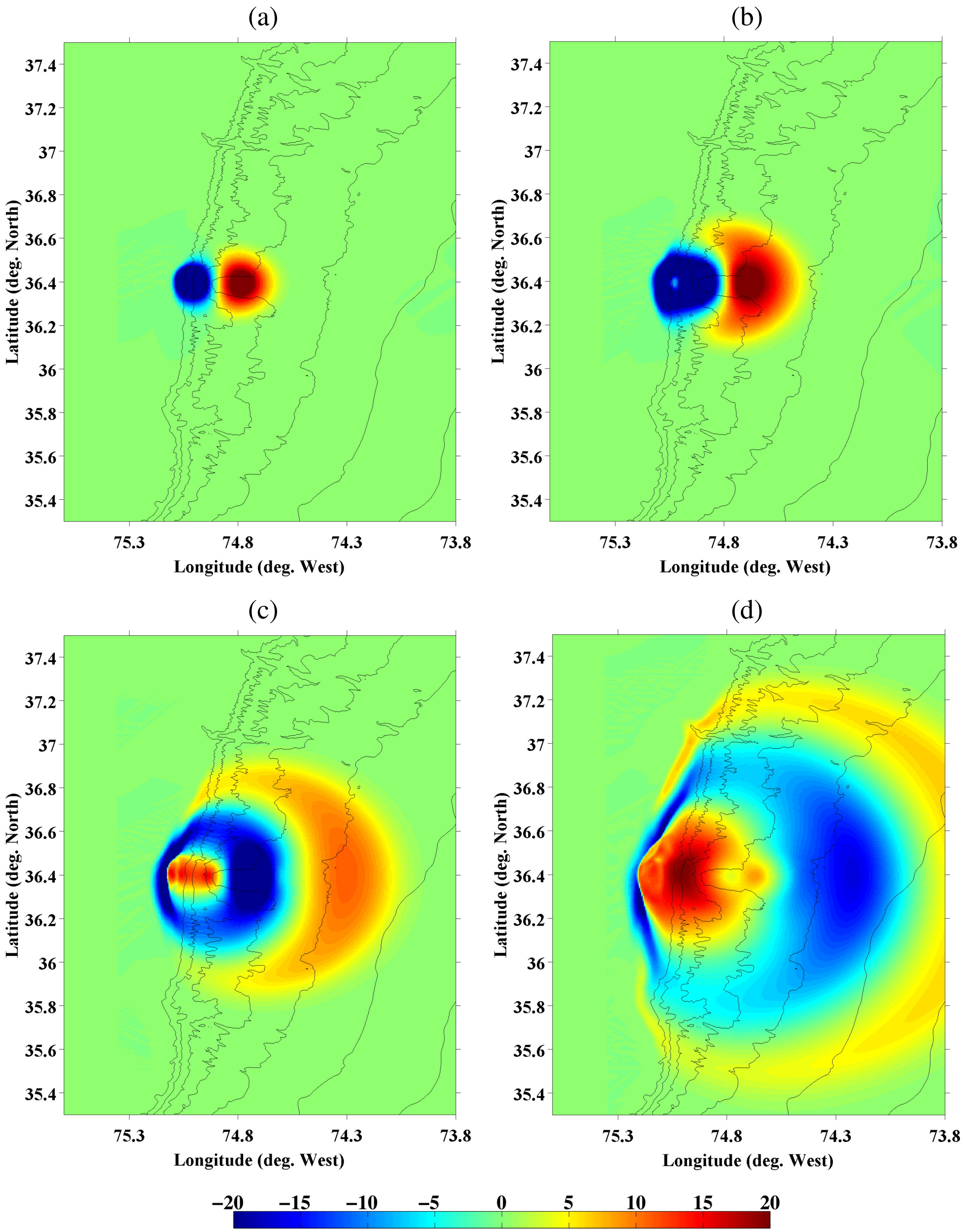


**Figure 8: Currituck SMF tsunami source geneartion in NHWAVE ($C_d$ = 0; 500 m grid). Instantaneous surface elevation (color scale is in meters) after: (a) 125 s; (b) 250 s; (c) 500 s; and (d) 800 s (13.3 min.) (see Figure 9 for E-W transects through these results).**

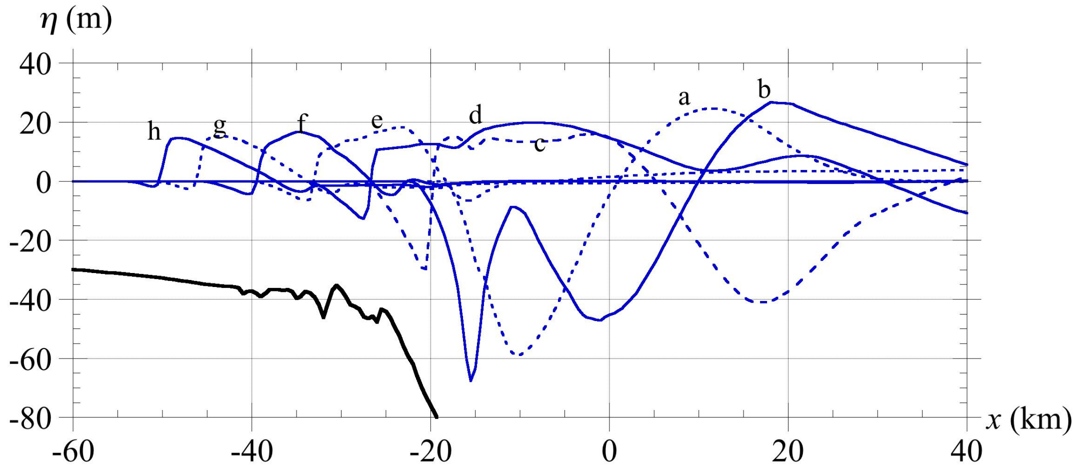


**Figure 9: Instantaneous surface elevation (---) in NHWAVE simulations of the Currituck SMF tsunami ($C_d$ = 0; 500 m grid, 3 sigma-layers), computed after: (a) 125 s; (b) 250 s; (c) 500 s; (d) 800 s (13.3 min); (e) 1100 s; (f) 1400 s; (g) 1700 s; (h) 2000 s (33.3 min). Results are shown along an E-W transect through the SMF center (36.39 N lat.), as a function of the distance to the center of the SMF; (---) denotes the ocean depth.**

The main bathymetry data base used to define the grid depth onshore of the failure is from USGS Coastal DEMs of the Northeast Atlantic Coast (3 arc-second resolution with a vertical accuracy on the order of 1 m). This grid is supplemented with ETOPO 1 data (1 arc-minute accurate) in deeper water, where necessary; the resulting bathymetry is plotted in Figure 1. Earlier sensitivity analyses (e.g., Grilli et al., 2013) have shown that a 500 m resolution with 3 sigma layers is adequate to ensure convergence of SMF tsunami source simulation results in NHWAVE. This is verified later for the present case.

Figure 8 shows the instantaneous surface elevation computed at various phase of the Currituck SMF tsunami source generation, up to 800 s (13.3 min.), slightly after the slump has stopped moving. Figure 8d shows that, at that time, surface elevation ranges between -20 and +20 m. Figure 9 shows surface elevations along an E-W transect through the SMF center, for these and other simulations at later times, up to 2000 s (33.3 min.). Figure 8 and Figure 9 show that, shortly after initiation of slide motion, at 125 s, the SMF source surface elevation takes the form of two inverted Gaussian humps located symmetrically above the initial slide location ($x$ = 0); this is qualitatively consistent with results of fully nonlinear potential flow computations for SMFs of idealized shape over a plane slope, described in Grilli et al. (1999, 2002, 2005, 2010a) and Watts et al. (2005).

Between 250 and 800 s, the same figures show that a negative elevation wave propagates onshore, followed by a “rebound” crest, and both of these waves transform through interactions with the continental shelf slope; this incoming wave trains thus initially looks like a so-called N-wave (Figure 9 curves b and c). During the same time period, a positive (Gaussian) elevation wave, initially generated in deeper offshore waters, propagates further offshore as a cylindrical wave of decreasing elevation. As shown by Geist et al. (2009), the northern part of this wave starts refracting over the shelf slope and propagating towards the Delaware Bay (Figure 8d); this will be detailed later by performing a computation in a larger domain. During interaction with the continental shelf slope, both shoaling and reflection of the incoming N-wave occur (see results at 500 and 800 s in the figures). At 800 s (13.3 min.), the maximum elevation reaches about 20 m. For later times (Figure 9 curves e to h), as the wave continues propagating onshore and over the shelf edge, the maximum height (trough to crest) of the incoming N-wave reaches about 23.5 m over the shelf after 1100 s, in a depth of about 35 m, before it starts decreasing as the wave spreads laterally (see results up to 2000 s). This decrease will be enhanced later by dissipation, first due to bottom friction and later to breaking; both of these dissipative effects will be modeled in FUNWAVE (see next section).

### Assessment of convergence of NHWAVE results

Here, we verify that a 500 m resolution grid with 3 sigma-layers is sufficiently accurate to compute the Currituck SMF tsunami generation with NHWAVE. Once this is assessed, these parameters will be used to simulate other SMF tsunami generation along the US East Coast. Thus Figure 10a,c shows instantaneous and maximum surface elevations computed with NHWAVE after 33 min., using a 250 m grid with 3 sigma-layers (i.e., doubling the horizontal resolution), and Figure 10bd shows the same simulation using a 500 m grid with 5 sigma layers (i.e., doubling the vertical resolution). These results can be visually compared with those of the reference computation in a 500 m grid with 3 sigma-layers, discussed before, and shown at 33 min. in Figure 11b,d. We see, the agreement is very good.

This agreement is better assessed in Figure 12, which shows E-W transects of computed surface elevations through the center of the SMF, for the same results. Figure 12a shows that refining the grid resolution by a factor of 2 yields very similar surface elevations but introduces a slight time shift in results; waves appear to be slightly slower in the finer grid. Figure 12b shows that increasing the number of sigma-layers from 3 to 5 yields slightly faster waves of similar surface elevation nearshore (although there appears to be slightly larger differences in elevation offshore). Finally, Figure 13 shows envelopes of maximum surface elevations computed along the same transect, for the various cases discussed above. Although there are larger differences over the continental shelf slope, as a function of discretization resolution and number of sigma-layers, nearshore, all maximum elevations are in good agreement.

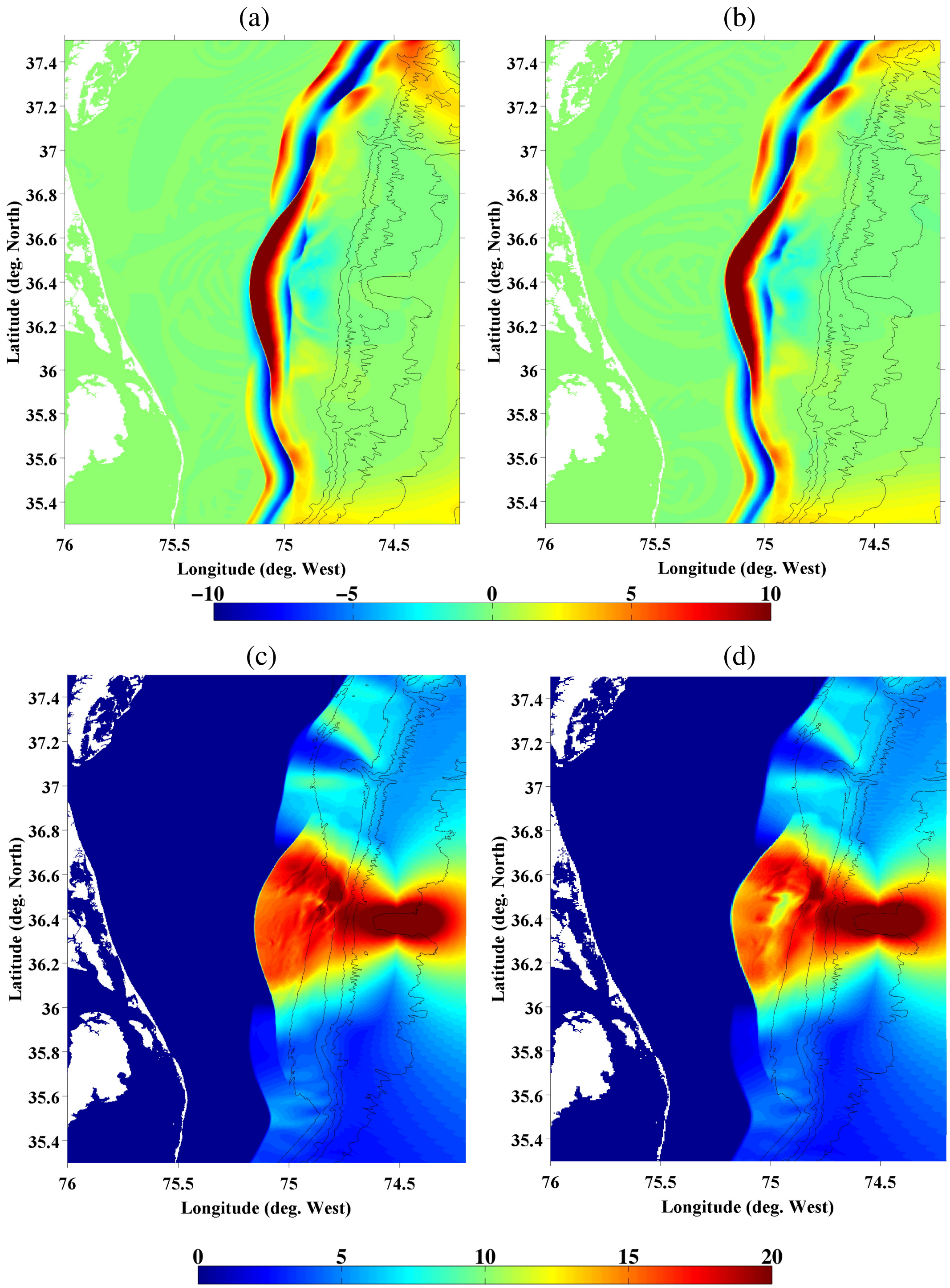


**Figure 10: Instantaneous (a,b) and maximum (c,d) surface elevation (color scale is in meters) computed after 2000 s (33.3 min.) of simulations of the Currituck SMF tsunami ($C_d$ = 0; same case as in Figure 8 and Figure 9), computed with NHWAVE, using: (a,c) a 250 m grid with 3 sigma-layers; or (b,d) a 500 m grid with 5 sigma-layers.**

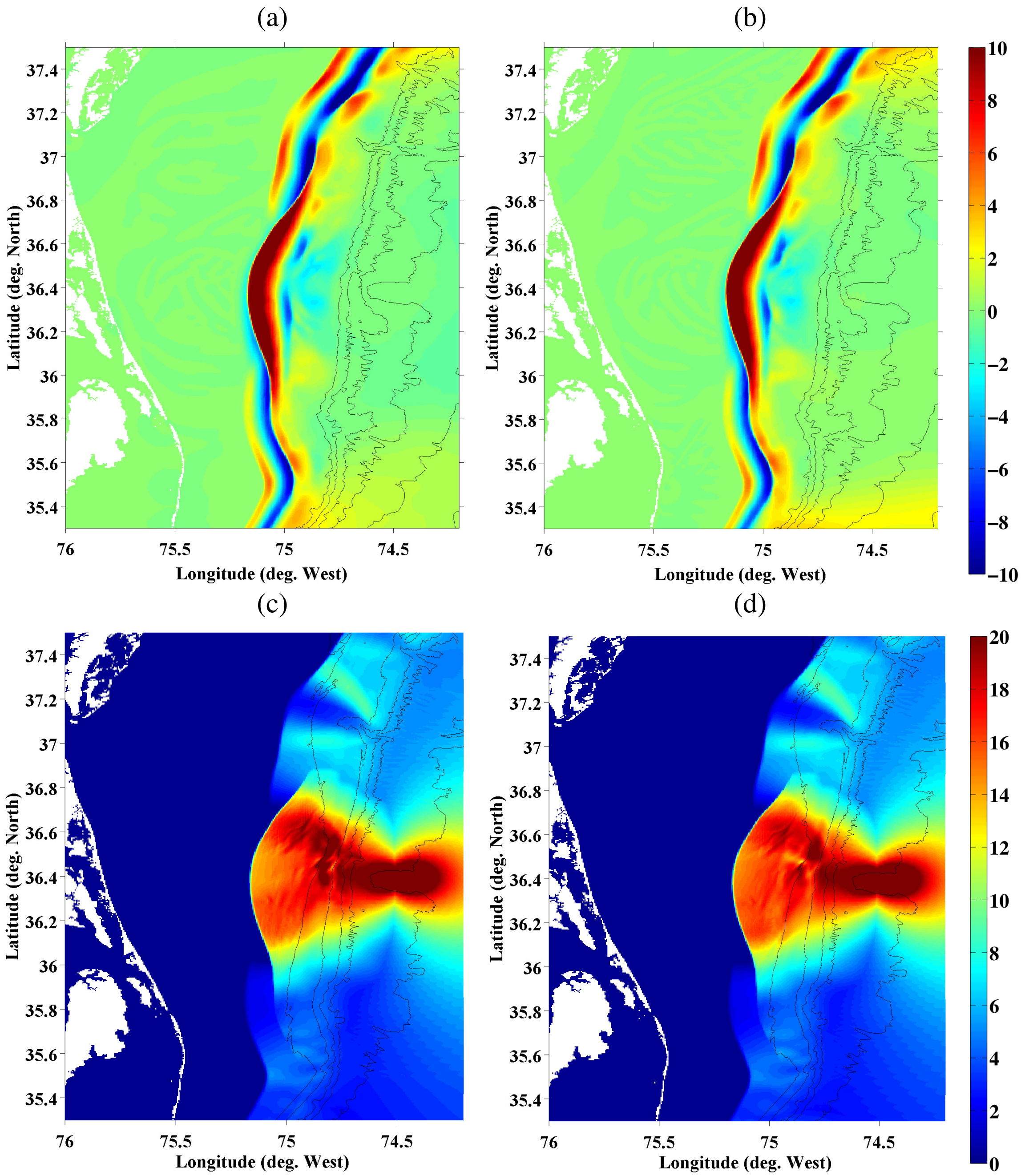


**Figure 11: Instantaneous (a,b) and maximum (c,d) surface elevation (color scale is in meters) computed after 2000 s (33.3 min.) of simulations of the Currituck SMF tsunami ($C_d$ = 0; 500 m grid), using: (a,c) FUNWAVE; (b,d): NHWAVE (with 3 sigma-layers). FUNWAVE results are initialized from NHWAVE results computed at 800 s (Figure 8). Results are shown over the zoomed in area marked in Figure 1.**

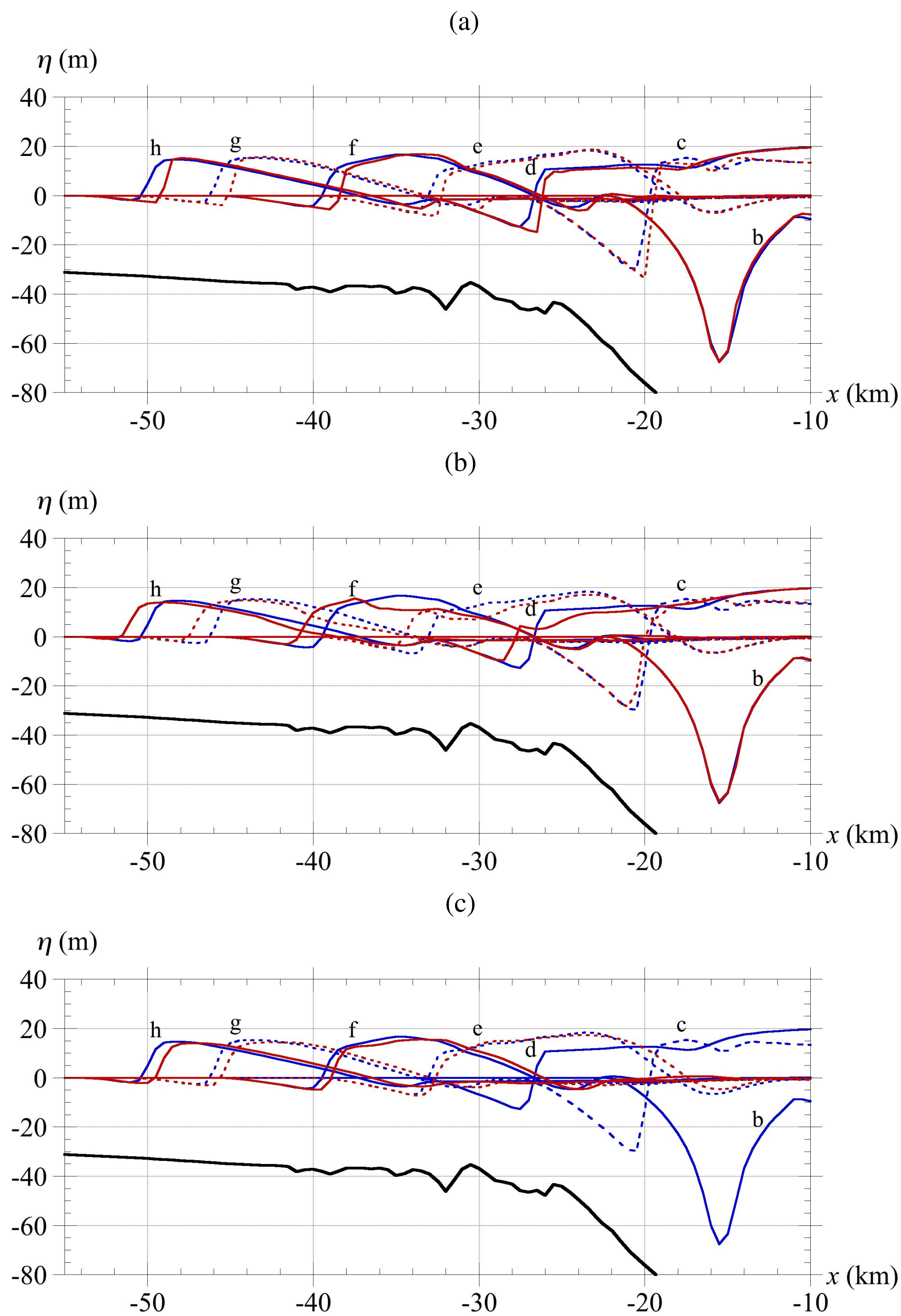


**Figure 12: Comparison of NHWAVE (500 m, 3 sigma-layers) surface elevations of Figure 9 (---) with those of (---): (a) NHWAVE on 250 m grid; (b) NHWAVE on 500 m grid with 5 sigma-layers; (c) FUNWAVE on 500 m grid initialized with NHWAVE 500 m grid results at 800 s (13.3 min.). We used $C_d$ = 0 and results are shown along an E-W transect through the SMF center (36.39 N lat.), as a function of the distance to the center of the SMF.**

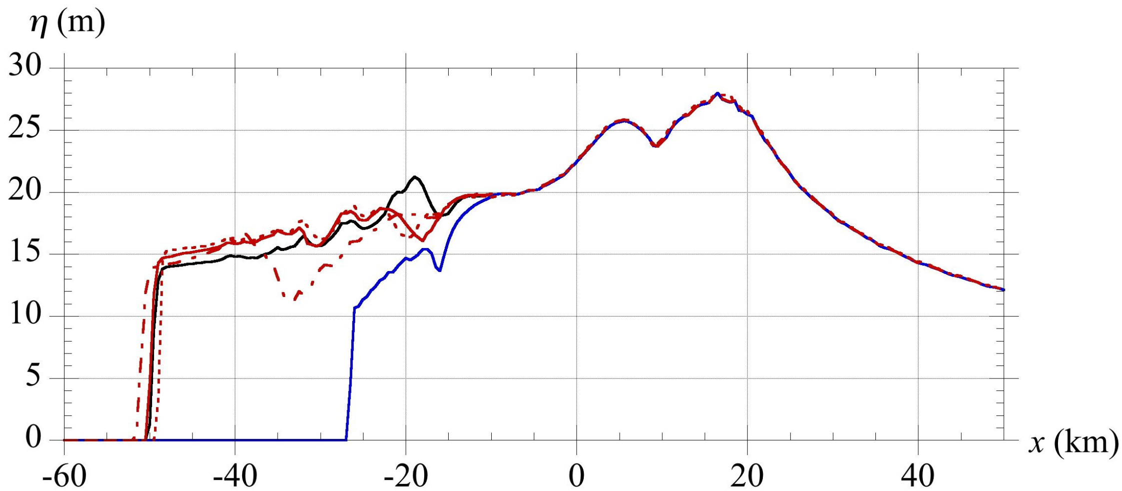


**Figure 13: Results of simulations of the Currituck SMF tsunami ($C_d$ = 0) along an E-W transect through the SMF center (36.39 N lat.), as a function of the distance to the center of the SMF. Maximum surface elevation after: 800 s (13.3 min.) in NHWAVE 500 m grid (---) (Figure 8), and 2000 s (33 min.) in FUNWAVE 500 m grid (---) (Figure 11c), NHWAVE 500 m grid (---) (Figure 11d), NHWAVE 250 m grid (- - -) (Figure 10c), and NHWAVE 500 m grid with 5 sigma-layers (-- - --) (Figure 10d).**

## Coupling of NHWAVE and FUNWAVE to simulate the tsunami early propagation

Based on the tsunamigenic duration of slide motion (Figure 7a), NHWAVE results are reinterpolated into a 500 m horizontal FUNWAVE grid, having the same footprint as the NHWAVE grid, soon after the end of slump motion, 800 s into the simulations (Figure 8d; i.e., surface elevation and horizontal velocity at the required depth of 0.513 the local depth, approximated by the middle sigma layer in NHWAVE).

Computations are then continued in FUNWAVE for later times, in the same 500 m regional grid domain as before (Figure 1). To prevent reflection at open boundaries, sponge layers are specified in FUNWAVE's domain over a width of 60 km or 120 grid cells inward from the northern and southern boundaries, and 100 km or 200 grid cells inward from the eastern boundary. These sponge layers do not fall within the zoomed in domain used to visualize results.

To assess the accuracy of the model coupling approach between NHWAVE and FUNWAVE, we first compared results of NHWAVE (run with 3 layers) simulations up to 2000 s (33.3 min.) to the corresponding FUNWAVE results, on the same 500 m grid. Figure 11 shows both the instantaneous and maximum surface elevations simulated in each model after 2000 s. Note, because no bottom friction can be specified in NHWAVE during tsunami generation, these simulations have been performed in FUNWAVE also assuming a bottom friction coefficient $C_d$ = 0. Because the tsunami is still in fairly deep water, however, this should not matter for results computed at this stage of propagation. In Figure 11, we see that, after 33.3 min., results of NHWAVE and FUNWAVE simulations are in good agreement. Figure 12c further compares intantaneous surface elevations computed in each model at various times and Figure 13 compares the maximum envelopes of surface elevation along an E-W transect passing through the SMF center. We again see that FUNWAVE and NHWAVE results obtained on the same grid (500 m reslution) are in good agreement, nearshore, over the continental shelf. On the transects of Figure 12c, we see that over the shelf, the surface elevations computed in both models appear to be closely identical, with FUNWAVE's results only lagging slightly in time as compare to NHWAVE results. Such a time lag, however, does not affect maximum inundation and runup.

The agreement between both FUNWAVE and NHWAVE results thus appears to be quite good, which justifies using this model coupling approach in all our future simulations in this work.

## FUNWAVE simulation of the Currituck SMF tsunami propagation to shore

### Coarse grid regional simulations

The same simulations are then run with FUNWAVE for a longer time in the 500 m grid (still initialized at 800 s from NHWAVE results). Now, however, we use the standard value of the bottom friction coefficient, $C_d = 0.0025$ in simulations.

Figure 14 first shows a sequence of instantaneous surface elevations computed up to $t$ = 99 min., at which time tsunami waves are impacting the coastline from North Carolina to Virginia Beach. We see that the onshore moving tsunami wavetrain propagates towards the shore as a series of long elevation and depression waves, as a result of dispersion. Specifically, between 82 and 99 min, the leading tsunami waves reach the entire shoreline of the barrier islands south of Virginia Beach, down to the outer banks of North Carolina, causing 5-6 m maximum wave elevations and overtopping the barrier at many locations (Figure 14c and d). After 99 min., 2-3 m elevation waves also reach the south of the Delmarva peninsula eastern shore and the mouth of the Chesapeake Bay (Figure 14d). Clearly, the 500 m grid is insufficient to accurately compute nearshore propagation and coastal tsunami impact. This will be done in computations in smaller and finer nested grids with 125 and 32 m resolutions, detailed below.

For validation, Figure 15 shows similar results computed for some of the same times by Geist et al. (2009). While there is an overall qualitative agreement between both studies, our results show more complex wave trains that also seem to be more influenced by the bottom bathymetry. Figure 16a further shows the maximum surface elevations computed in FUNWAVE, based on the same results, after 99 min., in a way that can be compared to similar results reported by Geist et al (2009), shown in Figure 16b. Again, a reasonable agreement is observed between both results.

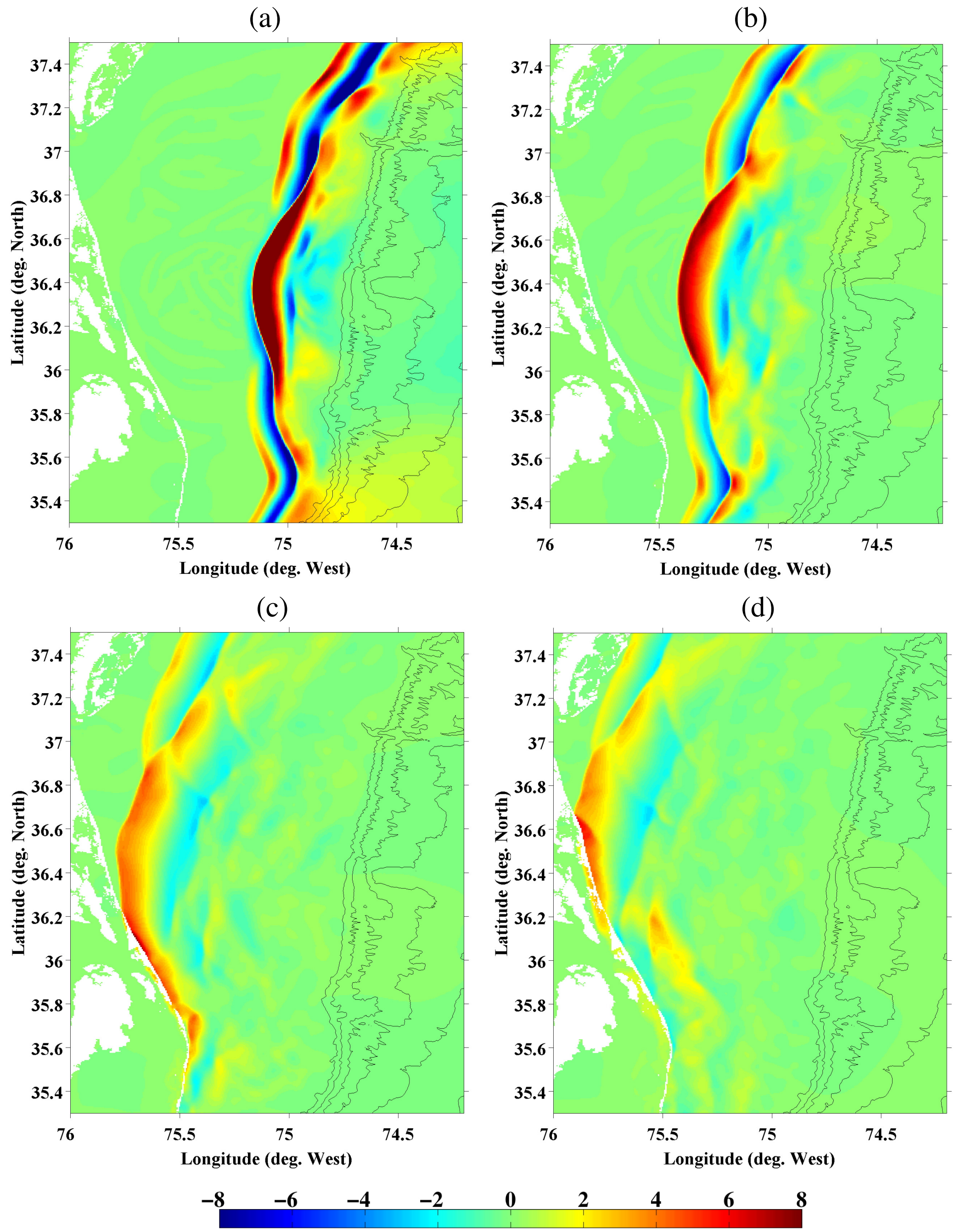


**Figure 14: Instantaneous surface elevation (color scale is in meters) in simulations of the Currituck SMF tsunami ($C_d$ = 0.0025; 500 m grid), computed in FUNWAVE initialized from NHWAVE results ($C_d$ = 0; 500 m grid; 3 sigma-layers) at 800 s (Figure 8), at *t* = (a) 33; (b) 49; (c) 82; and (d) 99 min. Results are shown over the zoomed in area marked in Figure 1**

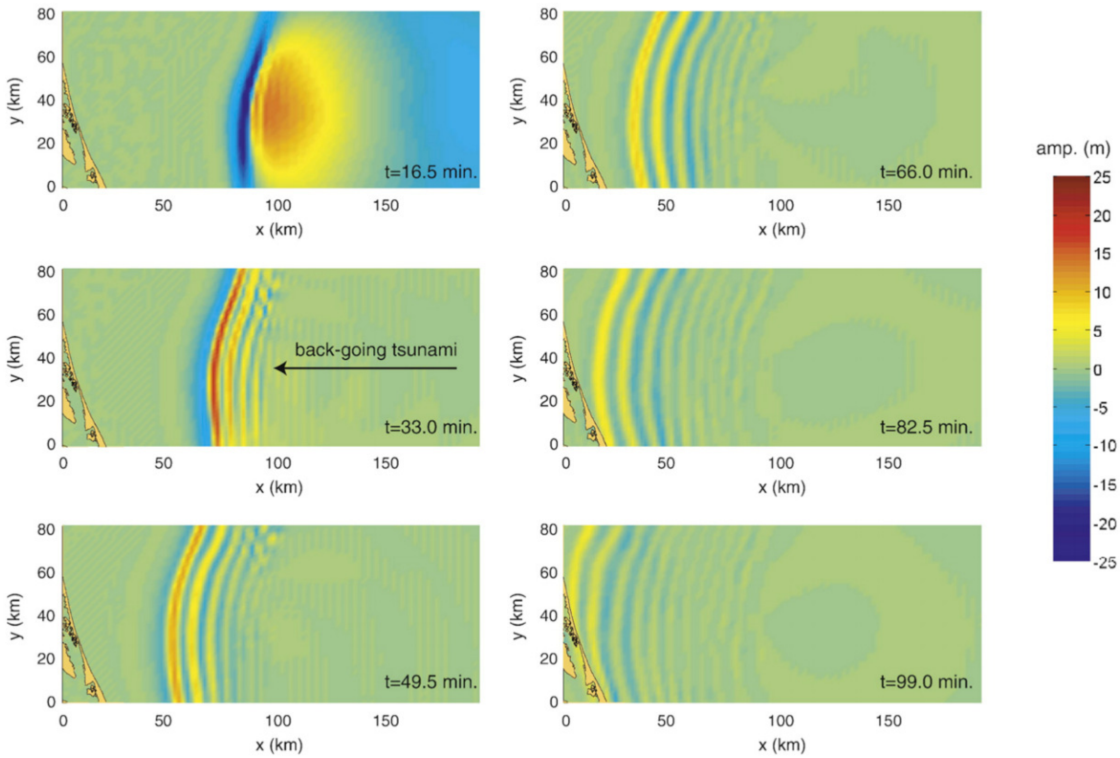


**Figure 15: Wave field computed by Geist et al (2009) as a function of time, during their Currituck SMF tsunami simulation.**

(a) (b)

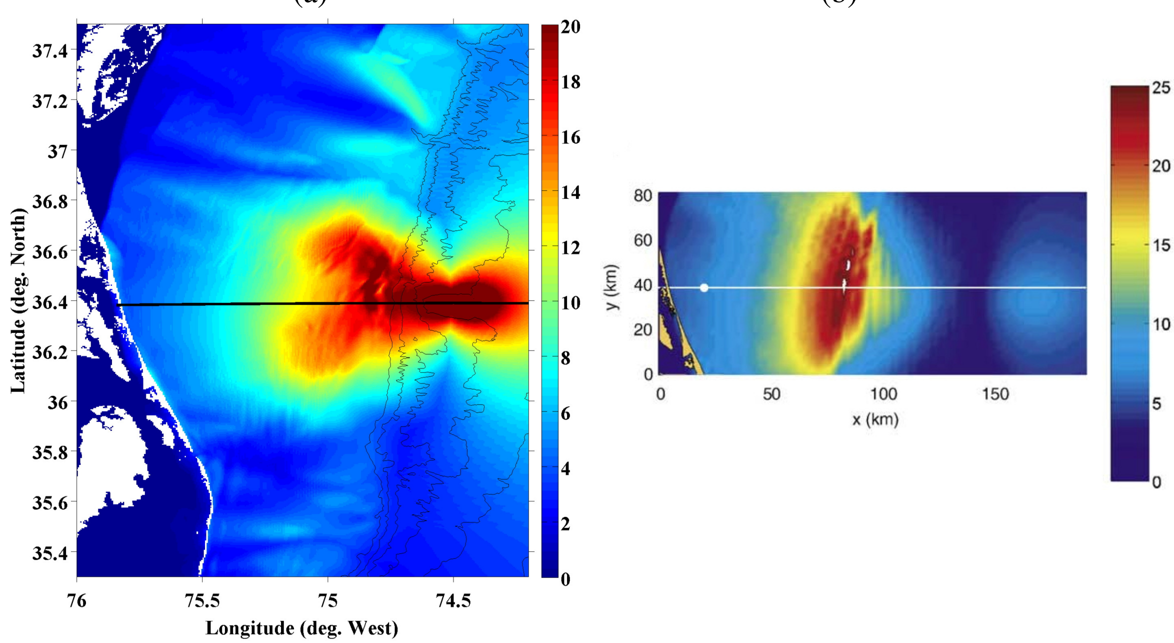


**Figure 16: Maximum surface elevation (color scales in meters) of the Currituck SMF tsunami, after 99 minutes of simulation: (a) FUNWAVE results; (b) from Geist et al. (2009). Horizontal lines mark transects through the SMF center.**

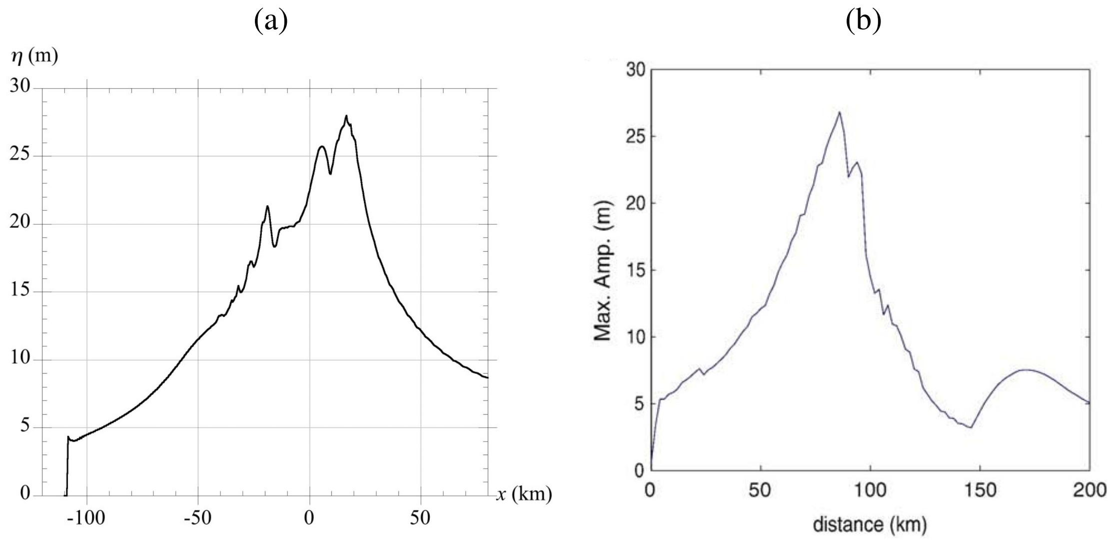


**Figure 17: Same results as in Figure 16, along E-W transects through the SMF center: (a) FUNWAVE results (as a function of distance to the SMF center) ; (b) from Geist et al. (2009).**

This is further confirmed in Figure 17, which compares the same results along an E-W transect through the SMF center (marked in Figure 16). While maximum surface elevations are in good agreement, we note that the spread of the surface envelope is wider in FUNWAVE results. The latter results also predict a longer characteristic wavelength of incoming waves than in Geist et al. (2009) and a slightly larger leading wave, relative to the rest of the incoming wave field. This longer wavelength and other differences in the generated incoming wave train result from differences in wave generation, which is performed here using the full 3D model NHWAVE while Geist et al. have used a semi-empirical SMF source.

Finally, in Figure 18, we computed the refraction of the generated tsunami more accurately on the northern shelf slope, in a larger FUNWAVE numerical domain, with identical 500 m resolution (800 by 800 km, using 1600 by 1600 grid, and $C_d$ = 0.0025; SW corner at 32.72 N 79.18 W), 100 km thick sponge layers on the Eastern boundary and 60 km on the southern and northern boundaries. Bathymetry and topography data are, as before, obtained from a combination of ETOPO-1 and regional DEMs data. Simulations are again initialized from NHWAVE (with 3 sigma-layers; $C_d$ = 0), in the same grid resolution, after 13.3 min. of simulations. Figure 18 shows results computed at 55 min where we see that initially offshore propagating waves to the North are bent by refraction into propagating over the shelf slope and shelf, resulting in potentially large tsunami impact along the coast of New Jersey from this source. This indicates that simulations in nested grids of SMF tsunami sources aimed at performing detailed inundation maps along the coast (performed at UoD) should be initiated in a large enough domain (such as used in Figure 18), in order to capture such additional wave refraction over the shelf slope and break.

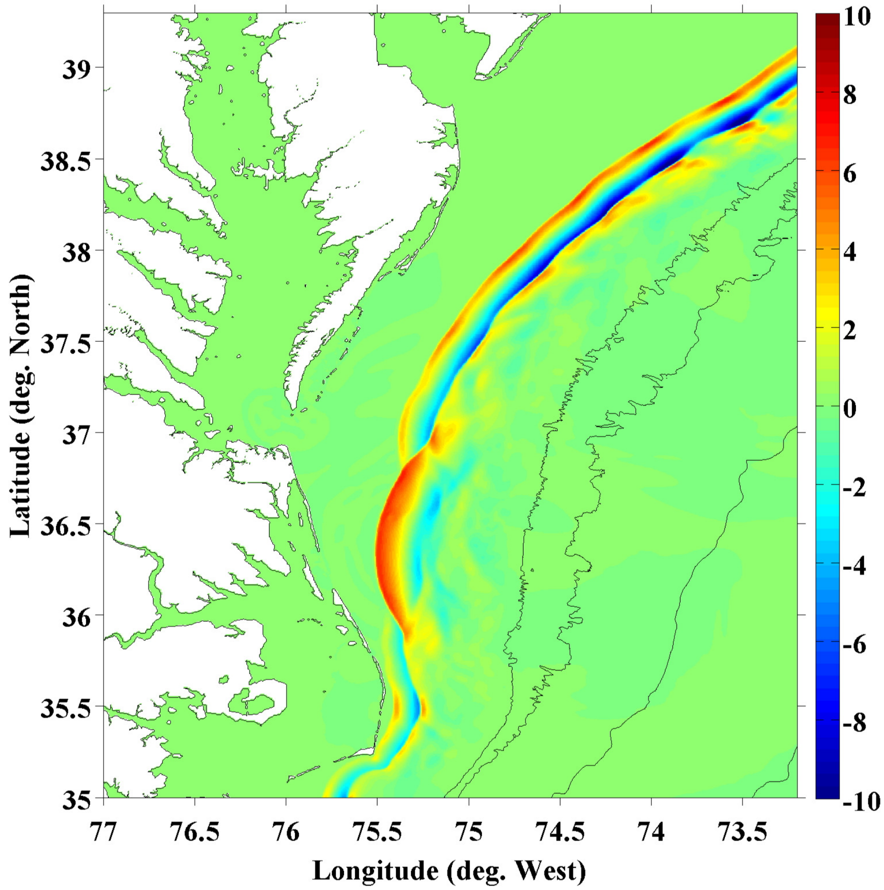


**Figure 18: Same computations as in Figure 14, but over a larger FUNWAVE 500 m grid, in order to better simulate refraction on the northern continental slope, off of New Jersey.**

## Fine grid nearshore simulations off of Virginia

Finally, since future NTHMP work in FY13 will involve more detailed simulations in the area of Norfolk, Virginia Beach (36.8 N) and the mouth of the Chesapeake Bay (37 N). Here, we performed one additional FUNWAVE simulation of the Currituck slide in a 125 m resolution nested grid located West of the source area, initialized from simulations in the 500 m grid used earlier (shown in Figure 1). This is discussed here.

Figure 19 shows the footprint of the 900 by 800, 500 m FUNWAVE grid (Figure 1) used so far with within it the boundary of the 125 m grid (with 1997 x 3197 meshes, 160 by 400 km), whose SW corner is located at 76.8 W and 34.6 N, similar to the 500 m grid. Sponge layers for this finer grid are 60 km thick on the eastern boundary, and 50 km thick on the northern and southern boundaries. Simulations in this grid were simply initialized from reinterpolating 500 m resolution results, once they had sufficiently entered the grid. This was deemed acceptable at $t$ = 26.6 min., which is the time of the instataneous surface elevation shown in Figure 19, which was computed in the 500 m grid. As we shall see in simulation results, in the finer 125 m grid, the northern and southern tsunami wave tails are easily damped in the sponge layers, while the main westward propagating tsunami waves, which dominate hazard for Virginia Beach and Chesapeake Bay, are not affected. Finally, Figure 19 also has a black box marked (76.5-75 W and 35.5-38 N) representing the zoomed in area used in later figures showing 125 m results, centered around Virginia Beach and the mouth of the Chesapeake Bay.

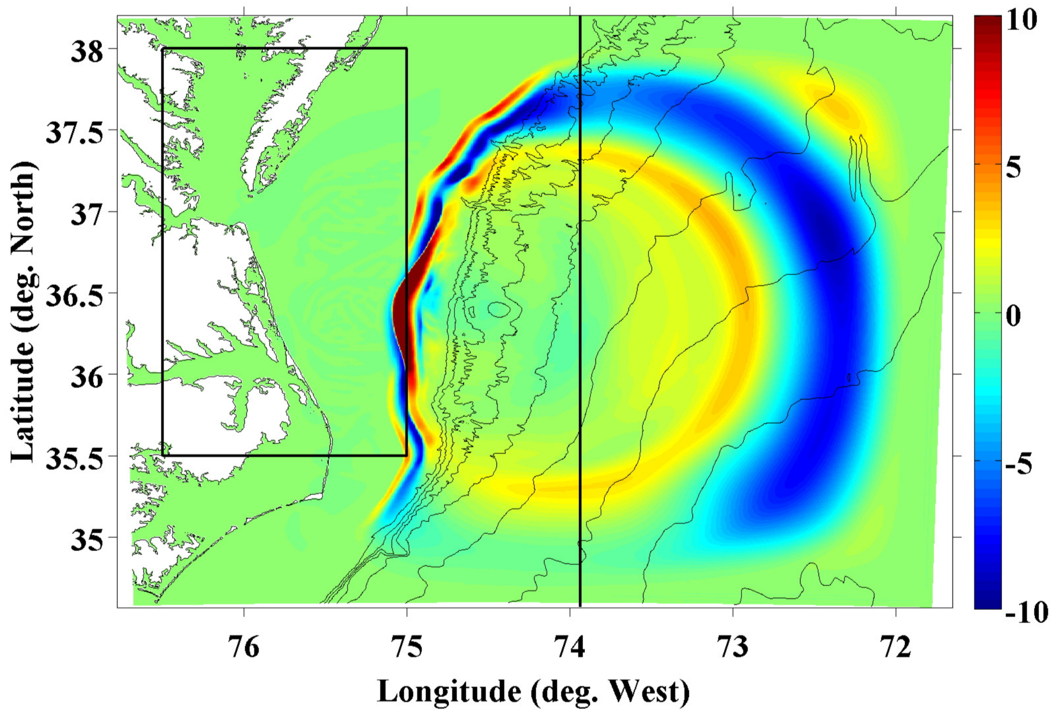


**Figure 19: Free surface elevation (color scale is in meters) in simulations of the Currituck SMF tsunami, computed with FUNWAVE in the 500 m grid (Cd = 0.0025) at t = 26.6 min., initialized at 13.3 min. from NHWAVE 500 m grid results. Computations in the finer FUNWAVE 125 m nearshore grid domain (to the left of the black line at 73.9 W) are initialized at this time by re-interpolating the 500 m results. The black box is the zoomed in area used in figures showing 125 m results, centered around Virginia Beach (36.9 N) and the mouth of the Chesapeake Bay (37 N).**

Results of simulations in the 125 m grid are shown in Figure 20 to Figure 23. Figure 20 shows a time sequence of instantaneous free surface elevation computed from $t =$ 26.6 to 200.6 min. We see, over this time, the tsunami propagates both westward towards the North Carolina and Virginia Beach coastline as well as NW into the Chesapeake Bay.

We note that Figure 20b approximately corresponds to the surface elevation computed in the 500 m grid shown in Figure 14c. Clearly, wave patterns and surface elevations look very similar although, as expected, more detail can be since in the 125 m grid results. The good agreement between results computed in the 125 m and 500 m grids is further confirmed in Figure 21, which compares results along an E-W transect through the SMF center (marked in Figure 20a). We see that differences are mostly a steeper front of the leading wave and higher-frequency oscillations in the trailing oscillatory tail of the tsunami wave train, in the 125 m grid results as compared to results in the 500 m grid.

Note that profiles (b,d,f) shown along the transect correspond to the times of Figure 20a,b,c, respectively.

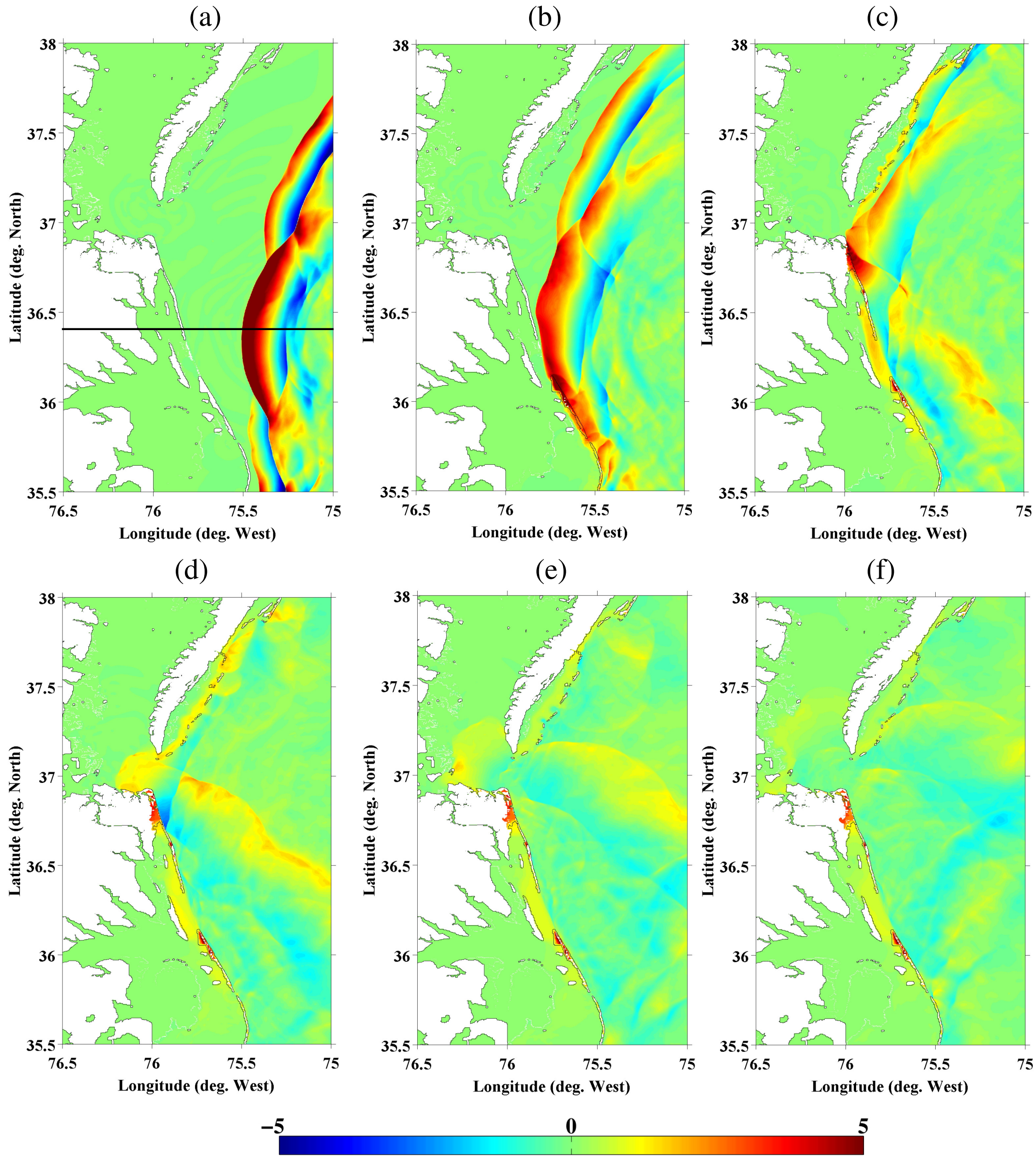


**Figure 20: Instantaneous surface elevation (color scale is in meters) in simulations of the Currituck SMF tsunami with FUNWAVE ($C_d$ = 0.0025) in the 125 m grid (Figure 19), initialized from FUNWAVE 500 m grid results ($C_d$ = 0.0025) at 26.6 min., shown at $t$ = (a) 56.6; (b) 86.6; (c) 116.6; (d) 146.6; (e) 176.6; and (f) 200.6 min. Results are shown over the zoomed in area marked in Figure 19. Black solid line in panel (a) marks East-West transect.**

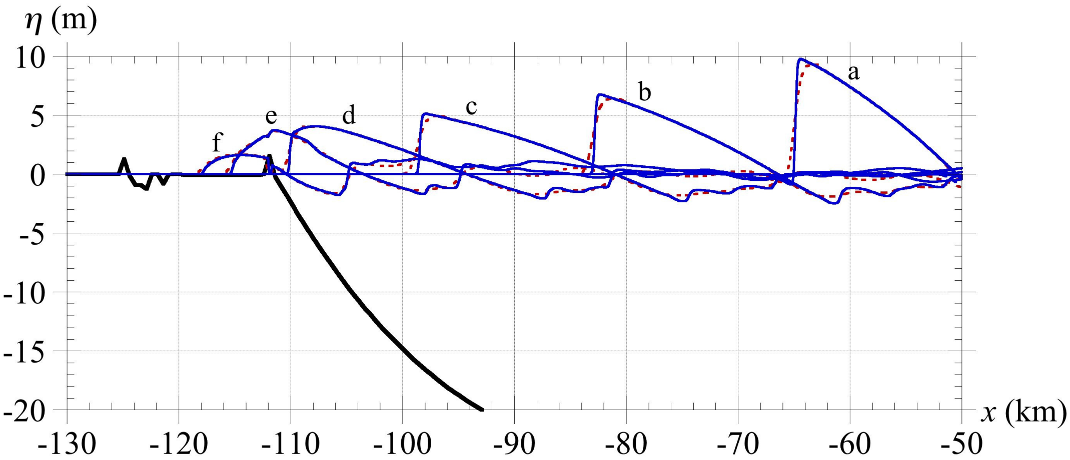


**Figure 21: Comparison of instantaneous surface elevations computed in FUNWAVE, in 125 m (---) or 500 m (- - -) grids, for the Currituck SMF tsunami simulations ($C_d$ = 0.0025) initialized at 13.3 min. from NHWAVE 500 m grid results. Surfaces are computed at $t$ = (a) 41.6; (b) 56.6; (c) 71.6; (d) 86.6; (e) 101.6; and (f) 116.6 min., along an E-W transect through the SMF center (36.39 N lat.; Figure 20), as a function of the distance to the center of the SMF; (---) denotes the ocean depth.**

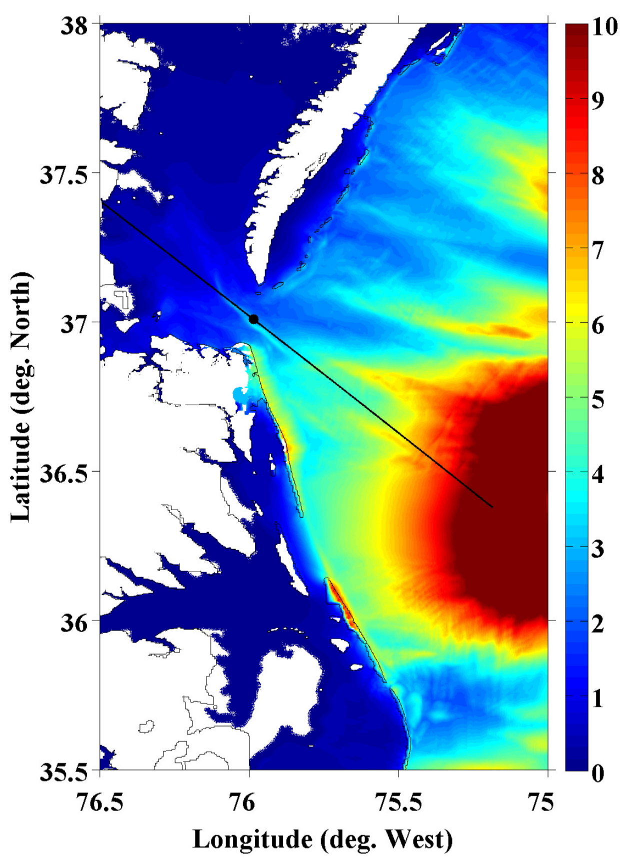


**Figure 22: Maximum surface elevation (color scale is in meters) in simulations of the Currituck SMF tsunami with FUNWAVE ($C_d$ = 0.0025) in the 125 m grid (Figure 19, Figure 20). Results are shown over the zoomed in area marked in Figure 19. Black line marks the location of transects with results shown in Figure 23 ($x$ = 0 marked by a black dot).**

More specifically, in Figure 20 and Figure 21, we see that the entire barrier island to the south of Virginia Beach is impacted by waves over 5 m elevation, and overtopped. Maximum tsunami impact in Virginia Beach appears to occur after 116 min. (Figure 20c), with maximum surface elevations over 5 m, and the tsunami flooding inland from this time onward. For later times, significant waves are seen to enter and propagate into the Chesapeake Bay. In particular, refraction north of Virginia Beach appears to cause wave impact on the Norfolk area, with surface elevations of 2-3 m (Figure 20d). This is further confirmed in the maximum surface elevations shown in Figure 22, where we see the Virginia Beach-Norfolk area being flooded with 3-6 m inundation. Maximum surface elevation in the mouth of the Chesapeake Bay appears to reach about 2 m.

Tsunami propagation into the Chesapeake Bay is further analyzed by computing surface elevations as a function of time, along a transect into the Bay (marked in Figure 22). These are shown in Figure 23 for the same time sequence as shown in Figure 20. While the tsunami elevation reaches nearly 7 m over the shelf, at the mouth of the Bay ($x$ = 0 here), it reduces to 2 m and then to 1 m, further into the shallow Bay. Because of the shallowness of the Bay, however, it is expected that an even finer nested grid (e.g., 30 m) may be needed to accurately compute tsunami propagation into the Bay (including impact in the Norfolk area). This will be the subject of FY13 work.

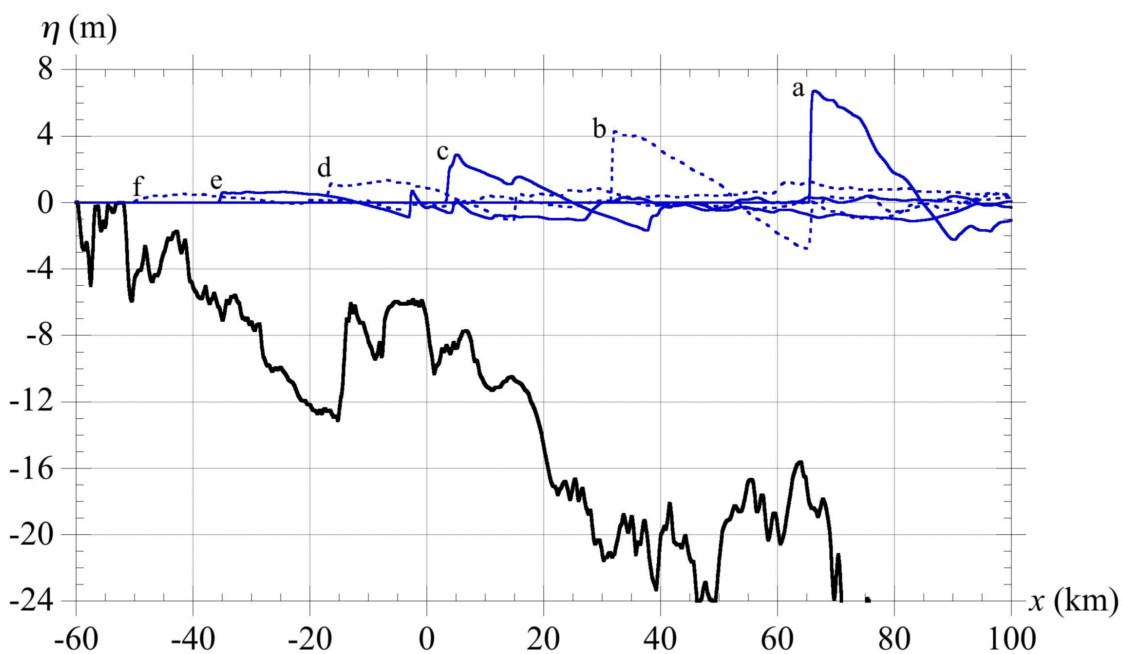


**Figure 23: Instantaneous surface elevation in simulations of the Currituck SMF tsunami with FUNWAVE ($C_d$ = 0.0025) in the 125 m grid (Figure 19), along the transect marked in Figure 22 ($x$ = 0 at the mouth of the Chesapeake Bay), at $t$ = (a) 56.6; (b) 86.6; (c) 116.6; (d) 146.6; (e) 176.6; and (f) 200.6 min.**

## SMF source Identification and simulations for NTHMP

As indicated in introduction, it was decided in this project and endorsed by the NTHMP Mapping and Modeling Subcommittee (MMS), to use a SMF similar to the historical Currituck slide (Figure 1) as a proxy to represent the potential worst case SMF scenario in the region of the US East Coast from Virginia to Cape Cod. Based on past work at URI (Grilli et al, 2009; Krause, 2011; Eggeling, 2012), this led to the selection of four areas with the potential for such a large SMF source, identified in Figure 24 as Study Areas 1 to 4, with areas 3 and 4 having the highest potential for tsunamigenic submarine landslides. Results from Grilli et al (2009) identify an increased tsunami risk in the Hudson River estuary and Western Long Island Coastline, likely corresponding to landslides occurring in Study Areas 1 and 2. Finally, the Cape Fear slide was selected as the worst case scenario SMF for the Myrtle Beach, SC coastline.

(a)

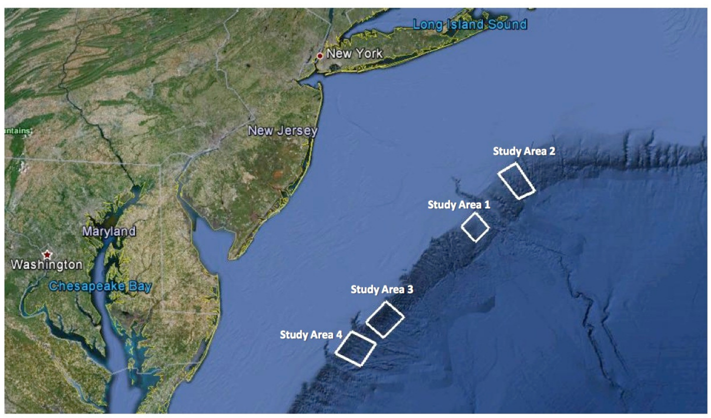


(b)

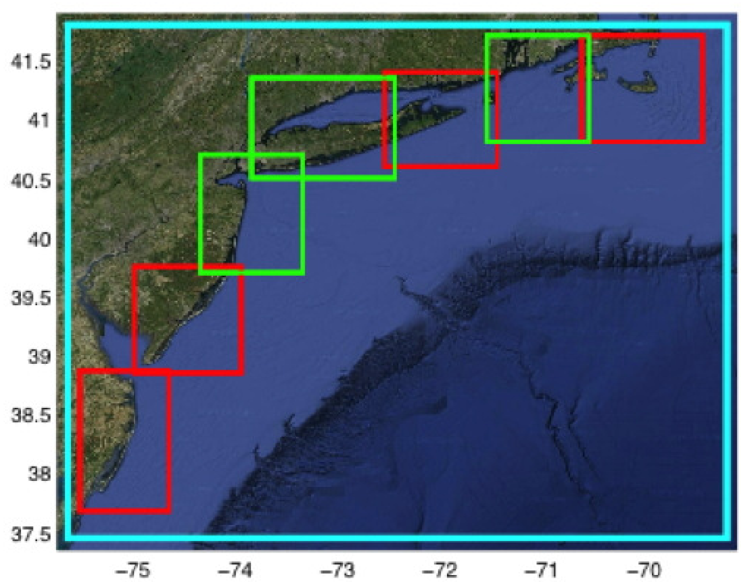


**Figure 24: (a) Areas identified for potential large SMF Sources North of Virginia; (b) Regional grid coverage for tsunami simulations along upper USEC.**

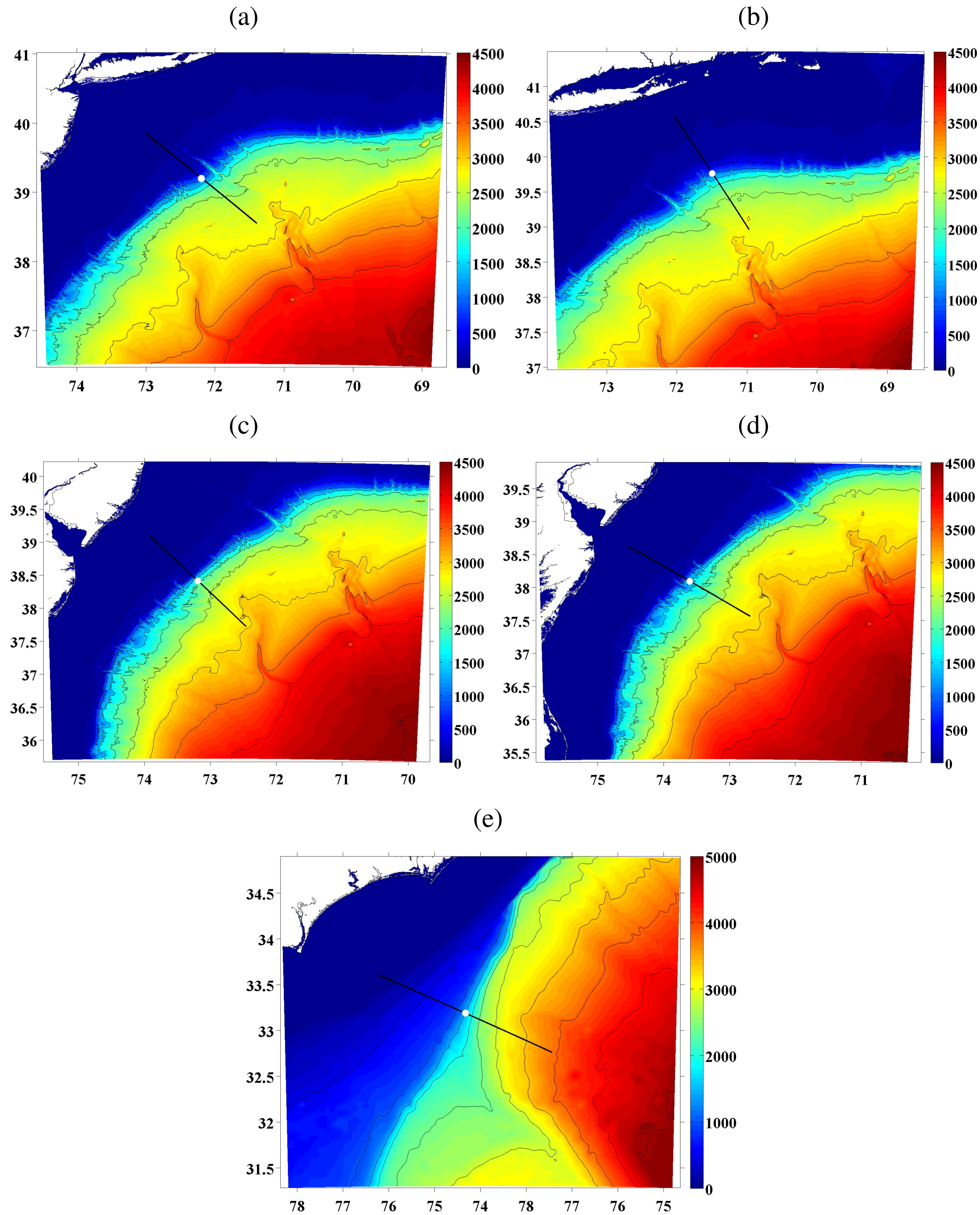


**Figure 25: Bathymetry (color scales in meters) and transects (----) through potential SMF areas (Figure 24): (a) Area 1; (b) Area 2; (c) Area 3; (d) Area 4 (historical Currituck slide); (e) Cape Fear Slide. Transects are shown in Figure 26 and white dots represent the initial location of each SMF. Axes denote West longitude and North latitude, respectively (degree).**

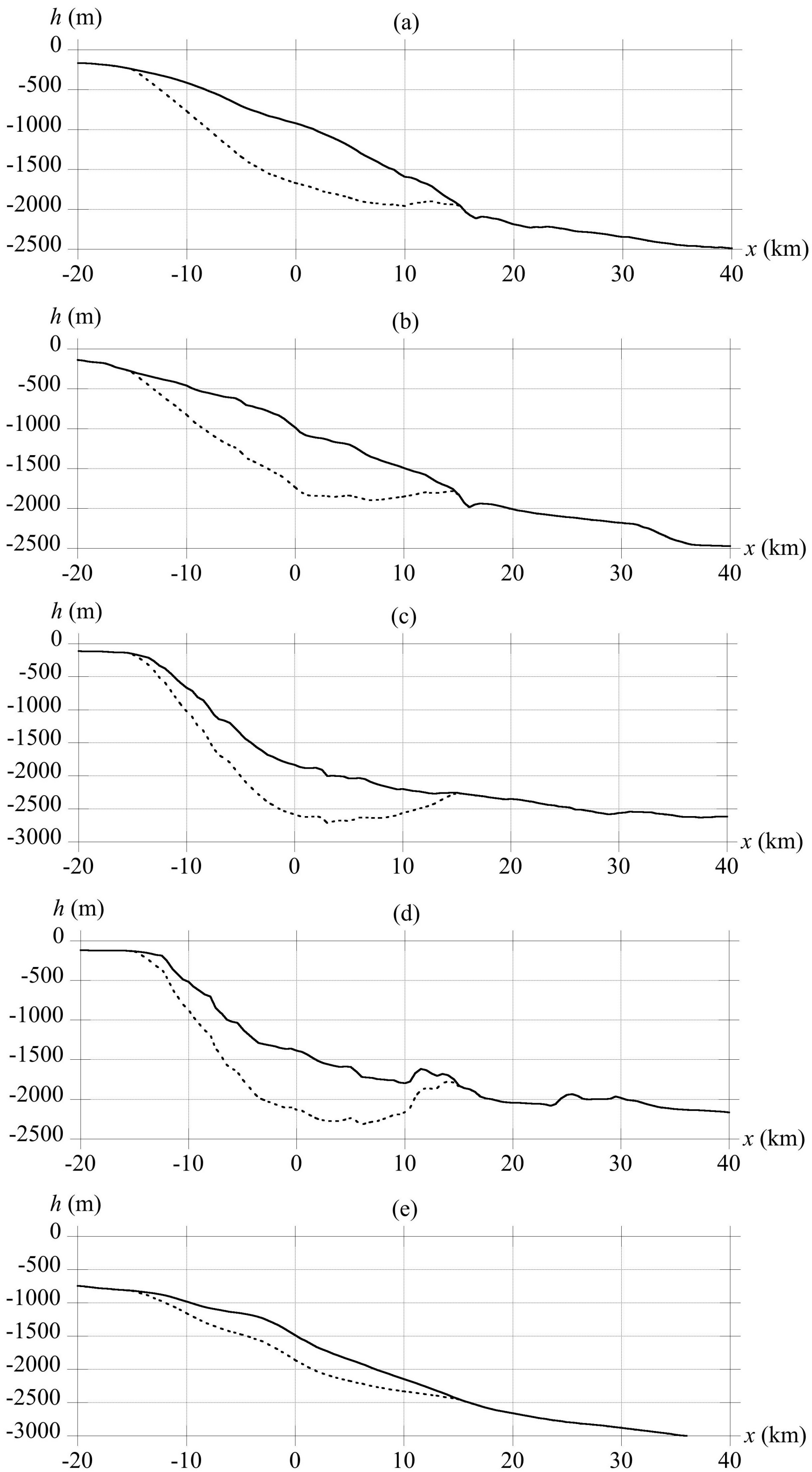


**Figure 26: Transects through potential SMF areas, as marked in Figure 25: (a) Area 1; (b) Area 2; (c) Area 3; (d) Area 4 (historical Currituck slide); (e) Cape Fear Slide. (----) bathymetry; (- - -) SMF cross section (at time $t = 0$ in simulations).**

## Sediment Availability in Study Areas 1-4

Study Area 1 is in the Hudson Apron, an area that is characterized by large soil deposits because it has experienced high sedimentation rates during the Pleistocene. Since most landslides along the U.S. Atlantic continental margin consist primarily of Quaternary sediment (a combination of Pleistocene and Holocene sediment), this site likely contains enough sediment for a Currituck volume slide to occur. Study Area 2 is located southwest of Ryan Canyon for which a cross slope survey (Eggeling, 2012) shows sufficient sediment available to cause a 20 km wide landslide. The area likely consists of appropriate sediment, thick enough for a Currituck landslide volume (Dr. Baxter, personal communication, URI).

Study Areas 3 and 4 are located near the Baltimore Canyon. Deep drilling by the USGS has found that there is a substantial thickness of Quaternary sediment present in the area (Dr. Chaytor, personal communication, USGS). However, in some places the thickness of this sediment does not exceed ~100 meters, as confirmed by perpendicular transects in these areas showing several hills 3 to 5 km wide with a vertical distance between peaks and valleys of roughly 200 to 400 meters (Figure 27). Determining the amount of sediment available for a Currituck size SMF at these locations is quite difficult, as the continuous action of down slope processes along the mid and north U.S. Atlantic margins leads to variable along slope thicknesses on a ridge to ridge scale (Dr. Chaytor, personal communication, USGS). Therefore, a landslide that may extend slightly deeper than the available sediment is constructed in these study areas, as this would represent multiple ridges failing at once and is consistent with the "worst probable scenario" objective of the NTHMP project.

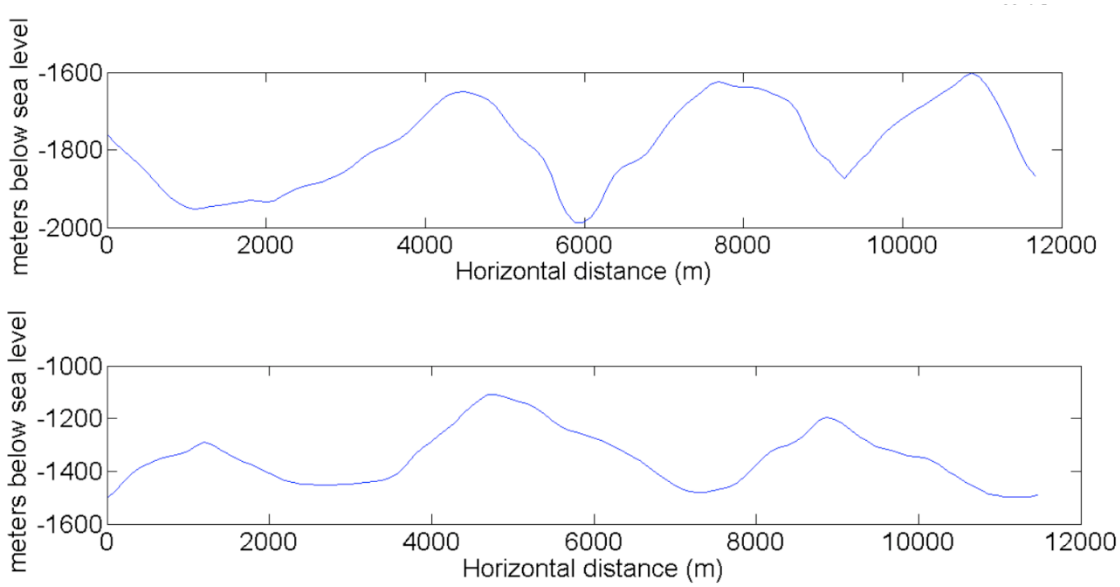


Figure 27: Cross slope bathymetry at sites 3 and 4 from Eggeling (2012).

## Parameterization of SMFs and tsunami sources in Study Areas 1-4

Figure 25a-d shows the bathymetry near and around the Study Areas 1-4 SMF simulation sites for the NTHMP project. Note, several small spurious steps in the bathymetry were observed and removed using a filtering function within Matlab, prior to performing tsunami simulations. The white dots in the figures mark the initial SMF center locations and the black lines are transects through each center, in the assumed azimuthal direction of slide motion $\theta$. Specific parameters for each slide, which correspond to Currituck proxies, as well as information on numerical grids are listed in Table 1. Similar to the Currituck slide event detailed before, the location of these 4 SMFs was selected to replicate the headwall of Slide 2 described in Locat et al (2009), where ~150 to 200 m of sediment were removed by the landslide at the 500 m post-excavation depth location. Based on these and the assumed Gaussian shape of each SMF (Figure 4 and Eqs. (1-2)), SMF cross-sections were constructed along each transect marked in Figure 25a-d, which are shown in Figure 26a-d.

Kinematics for each slide is given by Eqs. (3-6) based on parameters listed in Table 1; runout and total time of motion are given in Table 1. Based on these, NHWAVE (500 m grid and 3 sigma layers) was run for 13.3 min. for each case, leading to results shown in Figure 28a-d. We see that the initial wave features of each tsunami source are qualitatively identical, although there are differences in elevation and in dominant direction of propagation (as expected). These results were used by the UoD team to perform simulations in a series of finer nested coastal grids, in order to compute tsunami inundation maps; some of the regional grids used in these FUNWAVE simulations are shown in Figure 24b.

| | Currituck | Study Area 1 | Study Area 2 | Study Area 3 | Study Area 4 |
|---|---|---|---|---|---|
| **Grid lg. N (km)** | 400 | 500 | 500 | 500 | 500 |
| **Grid lg. E (km)** | 450 | 500 | 450 | 500 | 500 |
| **SW grid corner** | 34.6N 76.8W | 36.5N 74.6W | 36.9N 73.9W | 35.7N 75.5W | 35.4N 75.9W |
| **SMF $T$ (m)** | 750 | 750 | 750 | 750 | 750 |
| **SMF $b$ (km)** | 30 | 30 | 30 | 30 | 30 |
| **SMF $w$ (km)** | 20 | 20 | 20 | 20 | 20 |
| **SMF slope (deg.)** | 4 | 4 | 4 | 4 | 4 |
| **SMF Location** | 36.39N 74.61W | 39.19N 72.19W | 39.76N 71.49W | 38.41N 73.19 W | 38.09N 73.60W |
| **$\theta$ (deg. North)** | 90 | 136 | 153 | 140 | 126 |
| **$s_f$ (km)** | 15.8 | 15.8 | 15.8 | 15.8 | 15.8 |
| **$t_f$ (seconds)** | 710 | 710 | 710 | 710 | 710 |

**Table 1: Parameters of the actual Currituck SMF and of SMFs in selected areas 1-4**

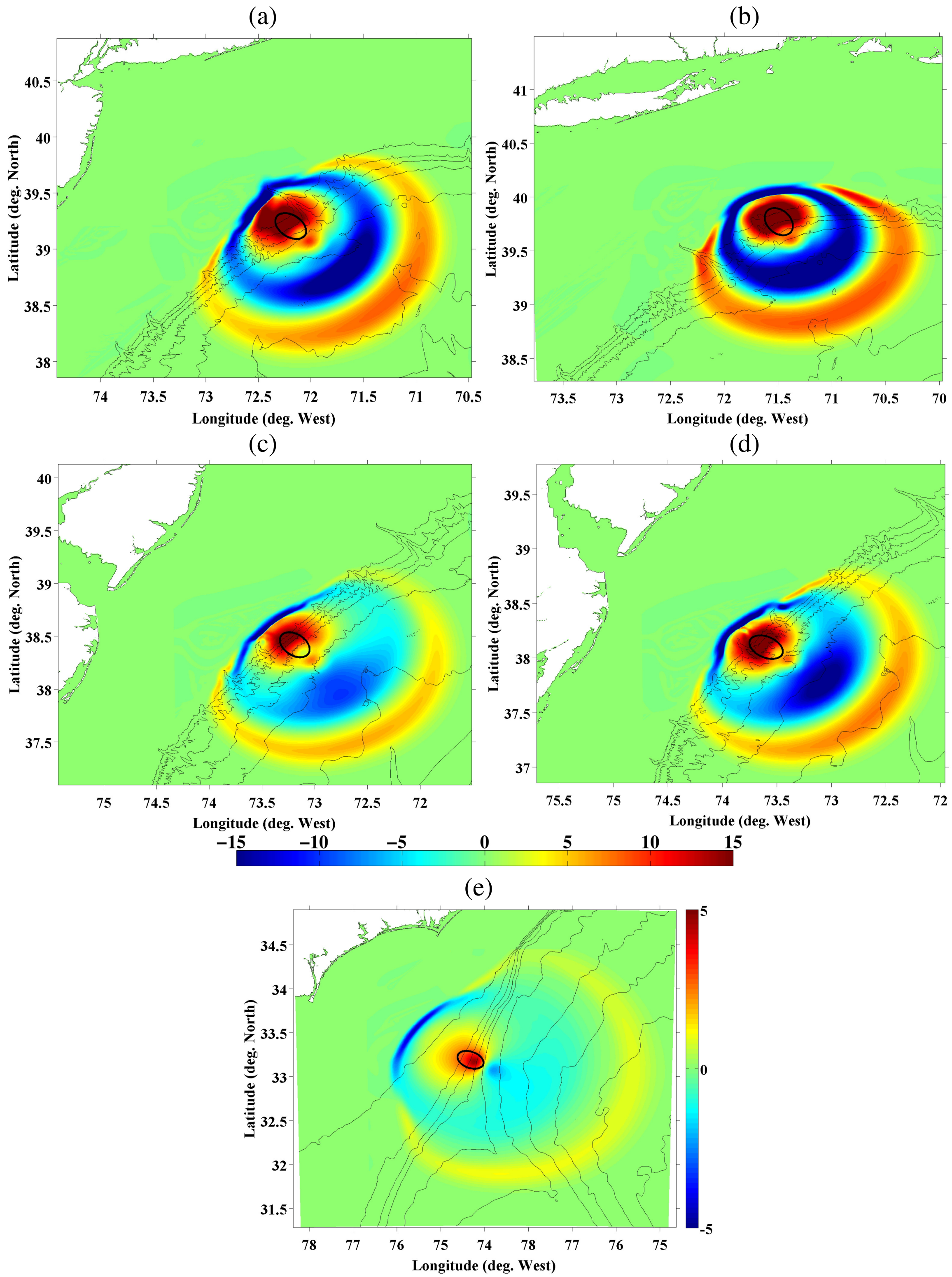


**Figure 28: Surface elevation of SMF tsunami sources in: (a) Area 1; (b) Area 2; (c) Area 3; (d) Area 4 (historical Currituck slide); and (e) Cape Fear Slide (Figure 24 and Figure 25), computed with NHWAVE (500 m grid, 3 sigma-layers, $C_d = 0$) at 13.3 min. (each SMF has stopped). Areas 1-4 sources are parameterized as Currituck proxies (Figure 26, Table 1).**

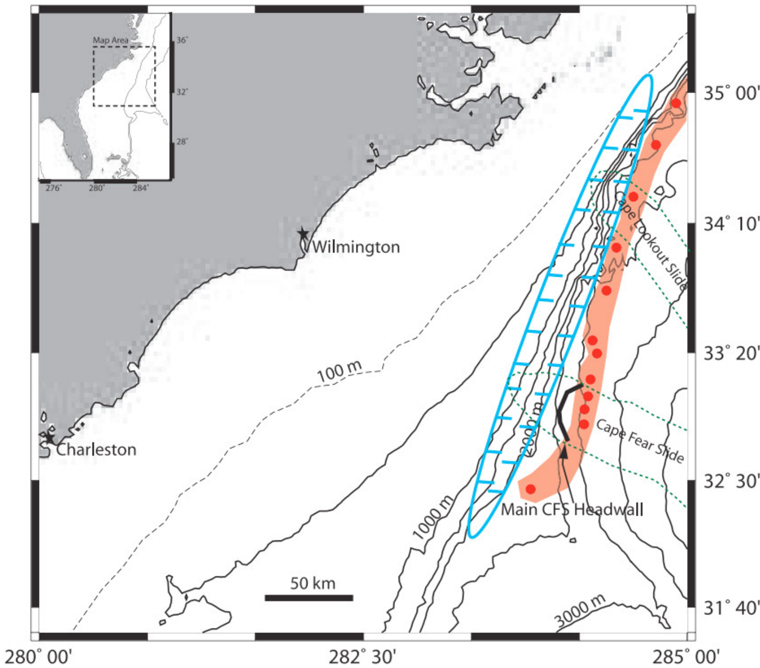


**Figure 29: General location of the Cape Fear Slide (CFS) headwall and debris field (Hornbach et al., 2007). The Carolina trough is outlined in blue and the approximate location of a chain of salt diapirs is denoted by red circles.**

## Parameterization of SMF and tsunami source in Myrtle Beach area

As indicated, the Cape Fear Slide (CFS) complex is used as a proxy for the extreme SMF tsunami source that would affect the Myrtle Beach, SC area. The CFS represents the most significant near-field tsunami hazard for the Myrtle Beach area as at least five major SMFs have occurred at this site over the past 30,000 years, some of which may have been associated with a significant tsunami (Hornbach et al. 2007). CFS is located approximately 200 km southeast of Cape Fear, NC, on the Carolina Trough, and intersects a normal fault at the main CFS headwall (Figure 29). Although the exact triggering mechanism for CFS events is poorly constrained, slope instability in the area may be facilitated by the extension of a normal fault at the site, salt intrusions, and gas hydrate dissociation within the sediment. As this fault remains active and salt intrusions are still present, the occurrence of a future tsunamigenic SMF in this region appears possible (Hornbach et al. 2007).

Hornbach et al (2007) identify 5 major escarpments exposed at the seafloor within the CFS complex, at depths ranging from about 890 m to 2300 m. They identify a normal fault located at roughly a 2500-3000 m depth, the Cape Fear diapir, and two emerging diapirs near the fault. All of the SMFs identified are landward of these and Hornbach et al (2007) conclude that the emergence of these diapirs, coupled with normal fault extension, steepens the adjacent sediment, possibly triggering slope failure.

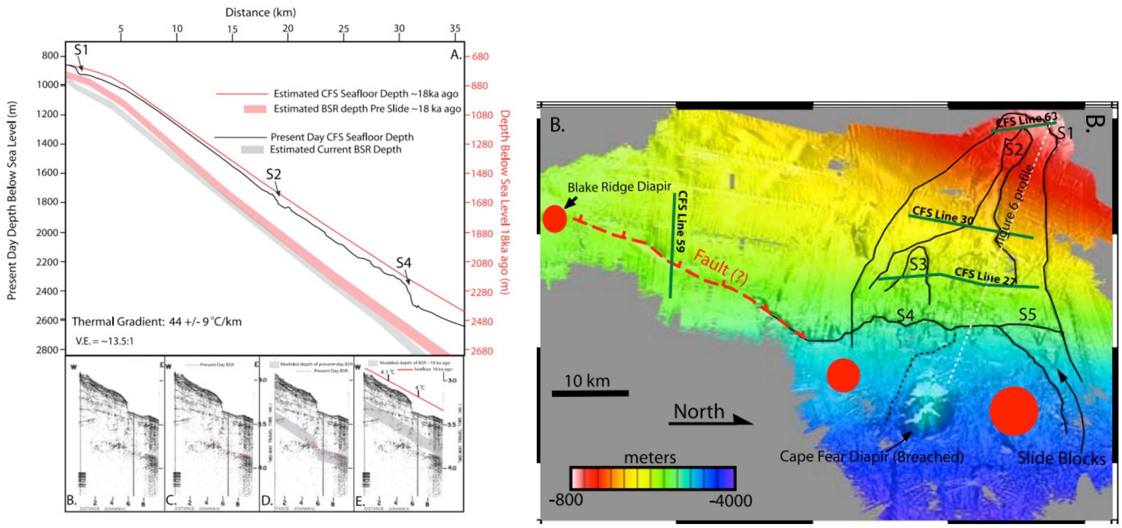


**Figure 30: (a) Transect showing the current bathymetry and identified SMF failure surfaces at the CFS site. (b) Bathymetry used in tsunami simulations, with SMF and diapir locations (red dots). (Hornbach et al., 2007).**

The base of gas hydrate deposits, indicated by bottom simulating reflectors (BSR) (Figure 30), represents a potential failure surface as a lowering of the threshold for mechanical failure may exist here (Flemings et al., 2003; Hornbach et al., 2004, 2007). Hornbach et al. (2007) also indicate that, in the future, warming oceans may contribute to further destabilizing of this boundary. Although many of the CFS SMFs likely did not occur along this surface, failure along the base of the gas hydrate deposits would result in a worst-case scenario SMF.

In the present simulations, a SMF of down-slope length $b$ = 30 km and width $w$ = 20 km, similar in horizontal footprint to the Currituck proxy SMFs (Table 1), was parameterized at the center of the CFS area, extending from about 800 m depth to about 2500 m depth (Figure 25e and Figure 26e). This parameterization is intended to represent a large portion of the CFS complex failing, as a result of the foot of the landslide, which is located roughly at the normal fault and diapirs, being destabilized and triggering a rapid retrogressive upslope failure, mobilizing the sediment above the BSR boundary. The previously used $T$ = 750 m maximum thickness of the Currituck SMF proxies is much thicker than that of both the SMFs observed at the CFS complex (roughly 100 m thick) and the depth of the BSR surface. Hence, a smaller SMF maximum thickness $T$ = 375 m was used here, intended to approximate failure along the upper limit of the BSR depth.

With these parameters and assuming a SMF slump motion (as for Currituck), which should lead to a worst case scenario tsunami source, Eq. (7) yields a characteristic time of motion $t_0$ = 320 s and a total time of motion $t_f$ = 1006 s (16.6 min.). As the characteristic distance of motion is not bounded in currently available data, it is assumed here that the CFS SMF has the same characteristic distance of motion as the Currituck SMF, i.e., about $s_0$ = 8 km, yielding a total SMF motion (runout) of $s_f$ = 15.8 km during the tsunamigenic period. This yields a maximum SMF velocity $v_{\max} = s_0/t_0 = 24.7$ m/s, which is consistent with the upper bound of measured slide velocities, based on cable breaks for low-density hemipelagic mud (Piper et al., 1999; Hornbach et al. 2007). [By contrast, matching the slump angle of rotation to that of Currituck ($\Delta\phi =$ □□□□□□□□) would yield a maximum SMF velocity of $v_{\max}$ ~ 50m/s, which is deemed too large.]

Hornbach et al. (2007) simulated two SMF generated tsunamis, using Grilli and Watts' (2005) and Watts et al.'s (2005) parameterization of the kinematics (which is similar to that used here). The larger of those SMFs had a maximum thickness $T = 120$ m, a width $w$ =50 km, and a down-slope length $b$ =10 km. Using a non-dispersive (NSWE) model (which is not recommended for landslide tsunamis), they simulated a maximum surface elevation of about 8 m at the 100-meter bathymetry line (Figure 31a), after about 30 min. of simulations. Although it does not feature dispersion and hence does not produce the proper number and height of generated waves, Hornbach et al.'s simulation is used for comparison with the present simulations of tsunami generation by the SMF parameterized, whose results are shown in Figure 31b.

NHWAVE is again applied over a 500 m resolution grid (using 3 sigma-levels). For the first 15 min. of simulations, our results appear qualitatively similar to those of Hornbach et al. (2007), except for the different main directionality. Differences in models used, however, as well as in slide parameters make a more detailed comparison of results impossible.

Results such as shown in Figure 31b will be used by the UoD team to compute additional nearshore propagation of the tsunami generated by the CFS SMF, using finer nested FUNWAVE grids, as well as tsunami inundation maps in the Myrtle beach area.

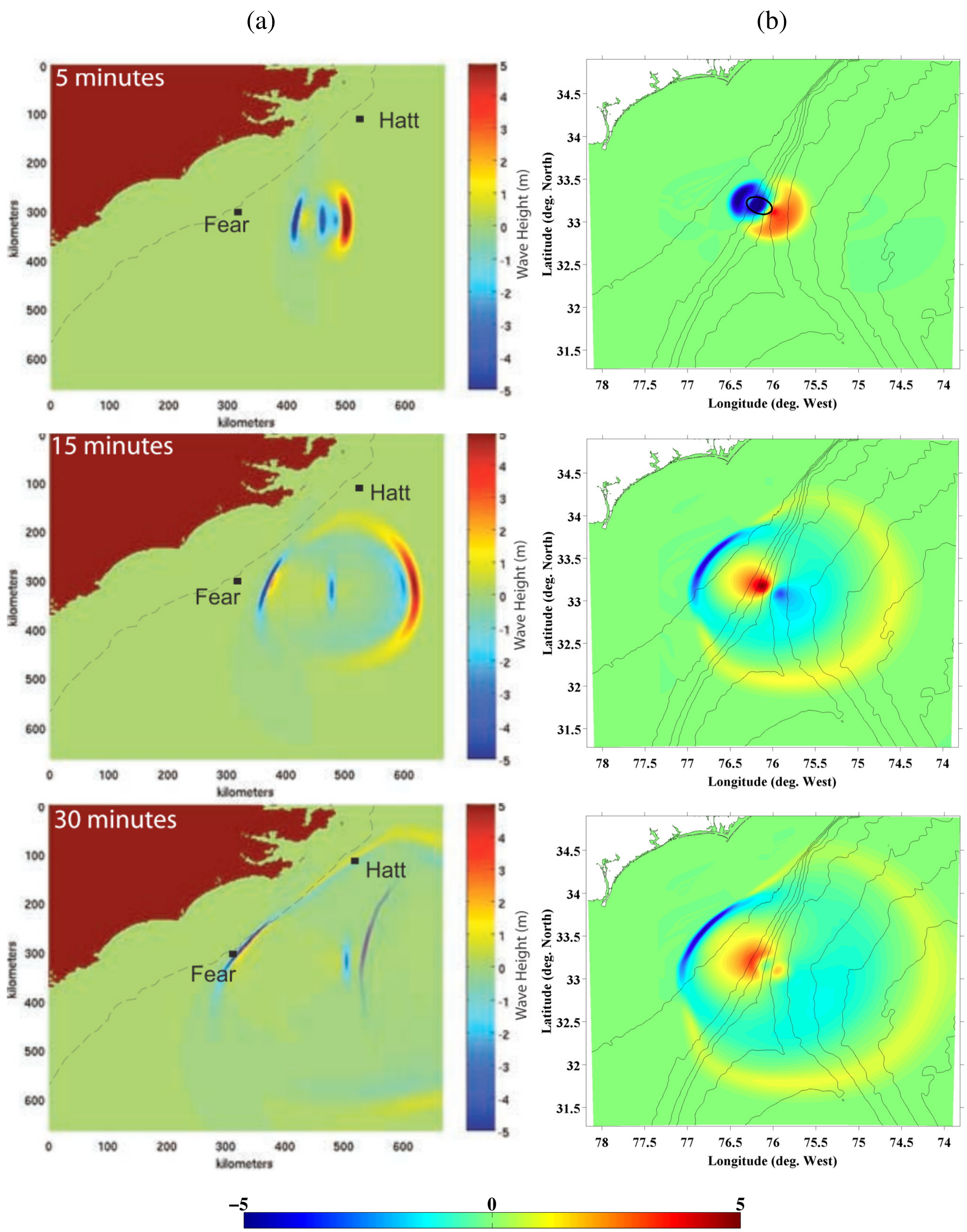


**Figure 31: CFS SMF tsunami source simulations. (a) Hornbach et al.'s (2007) tsunami (non-dispersive) simulations of their larger SMF (*T* = 120 m, *w* = 50 km, *b* = 10km). (b) NHWAVE simulations (500 m, 3 sigma- layers) of SMF in Table 1, at similar times except after 1100 s (18.3 min.) of simulations for the bottom figure, bottom color scale in meters.**

## References


Abadie, S., Morichon, D., Grilli, S.T. and S. Glockner 2010. Numerical simulation of waves generated by landslides using a multiple-fluid Navier-Stokes model. *Coastal Engineering*, **57**, 779-794.

Abadie, S., J.C. Harris, S.T. Grilli and R. Fabre 2012. Numerical modeling of tsunami waves generated by the flank collapse of the Cumbre Vieja Volcano (La Palma, Canary Islands): tsunami source and near field effects. *J. Geophys. Res.*, **117**, C05030.

Bunn, A.R. and B.A. McGregor 1980. Morphology of the North Carolina continental slope, Western North Atlantic, shaped by deltaic sedimentation and slumping. *Mar. Geol.*, **37**, 253–266.

Chaytor, J., ten Brink, A.R., Solow, J. and B.D. Andrews 2009. Size distribution of submarine landslides along the U.S. Atlantic Margin. *Mar. Geol.,* **264**, 16–27.

Eggelling, T. 2012. *Analysis of Earthquake Triggered Submarine Landslides at Four Locations Along the U.S. East Coast*. Masters Thesis, University of Rhode Island, 139 pps.

Enet, F, Grilli, S.T. and P. Watts 2003. Laboratory Experiments for Tsunamis Generated by Underwater Landslides: Comparison with Numerical Modeling. In *Proc. 13th Offshore and Polar Engng. Conf.* (ISOPE03, Honolulu, USA, May 2003), 372-379.

Enet F. and S.T. Grilli 2005. Tsunami Landslide Generation: Modelling and Experiments. In *Proc. 5th Intl. on Ocean Wave Measurement and Analysis* (WAVES 2005, Madrid, Spain, July 2005), IAHR Publication, paper 88, 10 pps.

Enet, F. and S.T. Grilli 2007. Experimental Study of Tsunami Generation by Three-Dimensional Rigid Underwater Landslides. *J. Waterway, Port, Coastal, and Ocean Engng.*, **133**(6), 442-454.

Flemings, P. B., X. L. Liu, and W. J. Winters 2003. Critical pressure and multiphase flow in Blake Ridge gas hydrates. *Geology*, **31**(12), 1057 – 1060.

Geist E., P. Lynett, and J. Chaytor 2009. Hydrodynamic modeling of tsunamis from the Currituck landslide. *Mar. Geol.,* **264**, 41-52.

Geist, E.L. and T. Parsons 2009. Assessment of source probabilities for potential tsunamis affecting the U.S. Atlantic Coast. *Mar. Geol.*, **264**, 98–108.

Grilli, A. and Grilli, S.T. 2013a. Far-field tsunami impact on the US East Coast from an extreme flank collapse of the Cumbre Vieja volcano (Canary Islands), draft report to NTHMP, in preparation.

Grilli, A and Grilli, S.T. 2013b. Modeling of tsunami generation, propagation and regional impact along the upper US East Coast from the Puerto Rico Trench. Draft report to NTHMP, in preparation.

Grilli, A. and Grilli, S.T. 2013c. Modeling of tsunami generation, propagation and regional impact along the upper US East Coast from the Azores convergence zone. Draft report to NTHMP, in preparation.

Grilli, S.T., Dias, F., Guyenne, P., Fochesato, C. and F. Enet 2010a. Progress In Fully Nonlinear Potential Flow Modeling Of 3D Extreme Ocean Waves. Chapter 3 in *Advances in Numerical Simulation of Nonlinear Water Waves* (ISBN: 978-981-283-649-6, edited by Q.W. Ma) (Vol. 11 in Series in Advances in Coastal and Ocean Engineering). World Scientific Publishing Co. Pte. Ltd., pps. 75- 128.

Grilli, S.T., S. Dubosq, N. Pophet, Y. Pérignon, J.T. Kirby and F. Shi 2010b. Numerical simulation and first-order hazard analysis of large co-seismic tsunamis generated in the Puerto Rico trench: near-field impact on the North shore of Puerto Rico and far-field impact on the US East Coast. *Natural Hazards and Earth System Sciences*, **10**, 2109-2125, doi:10.5194/nhess-2109-2010.

Grilli, S.T., Harris, J., F. Shi, J.T. Kirby, T.S. Tajalli Bakhsh, E. Estibals and B. Tehranirad 2013. Numerical modeling of coastal tsunami dissipation and impact. In *Proc. 33rd Intl. Coastal Engng. Conf.* (J. McKee Smith, ed.) (ICCE12, Santander, Spain, July, 2012), 12 pps. (in press). World Scientific Publishing Co. Pte. Ltd. http://www.oce.uri.edu/~grilli/ICCE12-grillietal.pdf

Grilli, S., Harris, J. and T. Tajalli Bakhsh 2011. *Literature Review of Tsunami Sources Affecting Tsunami Hazard Along the US East Coast*. NTHMP Progress report, CACR-11-08, Center for Applied Coastal Research, University of Delaware, 60 pps., http://chinacat.coastal.udel.edu/papers/grilli-etal-cacr-11-08.pdf

Grilli, S.T., Taylor, O.-D. S., Baxter, D.P. and S. Maretzki 2009. Probabilistic approach for determining submarine landslide tsunami hazard along the upper East Coast of the United States. *Marine Geology*, **264**(1-2), 74-97.

Grilli, S.T., Vogelmann, S. and P. Watts 2002. Development of a 3D Numerical Wave Tank for modeling tsunami generation by underwater landslides. *Engineering Analysis with Boundary Elements,* **26**(4), 301-313.

Grilli, S.T. and P. Watts 1999. Modeling of waves generated by a moving submerged body. Applications to underwater landslides. *Engineering Analysis with Boundary Elements,* **23**, 645-656.

Grilli, S. and P. Watts 2005. Tsunami Generation by Submarine Mass Failure, II: Modeling, Experimental validation, and Sensitivity Analysis. *J. Waterway, Port, Coastal, and Ocean Engng.*, **131**(6), 283-297.

Harris, J.C., S.T. Grilli, S. Abadie and T. Tajalibakhsh 2012. Near- and far-field tsunami hazard from the potential flank collapse of the Cumbre Vieja Volcano. In *Proc. 22nd Offshore and Polar Engng. Conf.* (ISOPE12, Rodos, Greece, June 17-22, 2012), Intl. Society of Offshore and Polar Engng., 242-249.

Hornbach, M.J., Lavier, L.L., Ruppel, C.D. 2007. Triggering mechanism and tsunamigenic potential of the Cape Fear Slide complex, U.S. Atlantic margin. *Geochemistry Geophysics Geosystems*, **8**(12).

Hornbach, M. J., D. M. Saffer, and W. S. Holbrook 2004. Critically pressured free-gas reservoirs below gas-hydrate provinces. *Nature*, **427**(6970), 142 – 144.

Krauss, T. 2011. *Probabilistic Tsunami Hazard Assessment for the United States East Coast*. Masters Thesis, University of Rhode Island, 132 pps., http://chinacat.coastal.udel.edu/nthmp/krause-ms-uri11.pdf.

Ma G., F. Shi, and J.T. Kirby 2012. Shock-capturing non-hydrostatic model for fully dispersive surface wave processes. *Ocean Modelling,* **43-44**, 22-35.

Locat, J., Lee, H., ten Brink, U.S., Twichell, D., Geist, E. and M. Sansoucy. 2009. Geomorphology, stability and mobility of the Currituck slide. *Mar. Geol.,* **264**, 28–40.

Piper, D. J. W., Cochonat, P. and M. L. Morrison 1999. The sequence of events around the epicentre of the 1929 Grand Banks earthquake: initiation of the debris flows and turbidity current inferred from side scan sonar. *Sedimentology,* **46**, 79–97.

Prior, D.P., Doyle, E.H. and T. Neurauter 1986. The Currituck Slide, Mid Atlantic continental slope-revisited. *Mar. Geol.,* **73**, 25–45.

Shi, F., J.T. Kirby, J.C. Harris, J.D. Geiman and S.T. Grilli 2012. A High-Order Adaptive Time-Stepping TVD Solver for Boussinesq Modeling of Breaking Waves and Coastal Inundation. *Ocean Modeling*, **43-44**, 36-51.

Tappin, D.R., Watts, P. and S.T. Grilli 2008. The Papua New Guinea tsunami of 1998: anatomy of a catastrophic event. *Natural Hazards and Earth System Sciences*, **8**, 243-266.

Twichell, D.C., Chaytor, J.B., ten Brink, U.S. and B. Buczkowski 2009. Morphology of late Quaternary Submarine Landslides along the U.S. Atlantic Continental Margin. *Mar. Geol,* **264**, 4–15.

ten Brink, U. S., D. Twichell, E. Geist, J. Chaytor, J. Locat, H. Lee, B. Buczkowski, R. Barkan, A. Solow, B. Andrews, T. Parsons, P. Lynett, J. Lin, and M. Sansoucy 2008. *Evaluation of Tsunami Sources with the Potential to Impact the U.S. Atlantic and Gulf Coasts*. Report to the Nuclear Regulatory Commission. USGS, 322 pps.

ten Brink, U. S., H. J. Lee , E. L. Geist, and D. Twichell 2009a. Assessment of tsunami hazard to the U.S. East Coast using relationships between submarine landslides and earthquakes. *Mar. Geol.*, **264**, 65–73.

ten Brink, U.S., R. Barkan, B.D. Andrews, and J.D. Chaytor 2009b. Size distributions and failure initiation of submarine and subaerial landslides. *Earth and Planetary Sci. Lett.*, **287**, 31–42.

ten Brink, U. S., D. Twichell, E. Geist, J. Chaytor, J. Locat, H. Lee, B. Buczkowski, and M. Sansoucy 2007. *The Current State of Knowledge Regarding Potential Tsunami Sources Affecting U.S. Atlantic and Gulf Coasts*. Report to the Nuclear Regulatory Commission. USGS, 166 pps.

Watts, S. T. Grilli, J. T. Kirby, G. J. Fryer, and D. R. Tappin 2003. Landslide tsunami case studies using a Boussinesq model and a fully nonlinear tsunami generation model. *Natural Hazards and Earth System Sciences*, **3**, 391-402.

Watts. P. Grilli, S., Tappin, D. and G. Fryer 2005. Tsunami Generation by Submarine Mass Failure, II: Predictive Equations and Case Studies. *J. Waterway, Port, Coastal, and Ocean Engng*., **131**(6), 298-310.